



**University of  
Zurich**<sup>UZH</sup>

# What impact do thin debris layer have on ablation for debris covered glaciers? A combined field- modeling study on Zmuttgletscher

GEO 511 Master's Thesis

**Author**

Simon Farsky  
15-737-273

**Supervised by**

Prof. Dr. Andreas Vieli  
Boris Ouvry

**Faculty representative**

Prof. Dr. Andreas Vieli

29.04.2022

Department of Geography, University of Zurich



---

## Abstract

Debris covered glaciers are commonly found in alpine environments. As a result of a protective debris layer, debris covered glaciers respond differently to changes in climate. Current numerical ablation models simulating debris covered glaciers, however, do not account for enhanced melt for thin debris layers as is proven by empirical data. Debris layers thinner than a specific critical debris thickness as well as partially covered surfaces are often found to have increased melt rates compared to clean ice. As current numerical models attribute insulation to debris layers of any thickness, it is of great importance to include enhanced melt for thin layers to analyse how surface mass balance is affected when enhanced melt is incorporated. In a first part, this study focuses on reproducing the Østrem curve with data collected during a field campaign on Zmuttgletscher. Partially covered surfaces were found to enhance melt by up to 20 % the clean ice melt rate, whereas insulating of thicker debris layers reduced surface melt by as much as 61 %, depicting an accurate Østrem curve. Melt rates were shown to be reduced on fully covered surfaces of any thickness, with melt rates decreasing as debris thickness increased.

In a second part, simulations of glaciers with and without enhanced melt for thin debris layers were compared and analysed. Step change experiments as well as sinus simulations revealed that, for a glacier building up with a simplified bed geometry, inclusion of enhanced melt for thin debris layers has no significant impact on surface mass balance. Differences increase with a higher selected enhancement factor but do not affect surface mass balance significantly. With an enhancement 1.6 times the clean ice melt rate for debris layers ranging from  $<0$  to 0.03 m thickness, differences stay insignificantly minimal and do not necessitate the need to implement enhanced melt in numeric melt models.

---

## Contents

<b>ABSTRACT</b> .....	<b>II</b>
<b>LIST OF FIGURES</b> .....	<b>IV</b>
<b>LIST OF TABLES</b> .....	<b>V</b>
<b>1 INTRODUCTION</b> .....	<b>1</b>
<b>2 STATE OF RESEARCH</b> .....	<b>4</b>
<b>3 METHODOLOGY</b> .....	<b>13</b>
3.1 STUDY AREA .....	13
3.2 FIELD MEASUREMENTS .....	14
3.3 MODELLING.....	16
<b>4 RESULTS</b> .....	<b>21</b>
4.1 FIELD MEASUREMENTS .....	21
4.1.1 <i>Image analysis</i> .....	21
4.1.2 <i>Debris coverage and albedo</i> .....	22
4.1.3 <i>Ablation Measurements</i> .....	24
4.2 MODELLING.....	30
4.2.1 <i>Step Change Simulation</i> .....	30
4.2.2 <i>Sinus Simulation</i> .....	32
4.2.3 <i>Gradual Increase of the ELA</i> .....	34
4.2.4 <i>ELA Forcing</i> .....	36
4.2.5 <i>Debris Layer Transport</i> .....	37
4.2.6 <i>Step change with different <math>D_0</math> of <math>D_0=0.1</math> m</i> .....	41
4.2.7 <i>Summary of modelling results</i> .....	43
<b>5 DISCUSSION</b> .....	<b>44</b>
5.1 IMPLICATIONS OF FIELD MEASUREMENTS .....	44
5.2 IMPLICATIONS OF MODELLING EXPERIMENTS .....	46
5.3 ADDITIONAL IMPLICATIONS .....	48
5.4 LIMITATIONS .....	50
<b>6 CONCLUSION</b> .....	<b>52</b>
<b>7 ACKNOWLEDGMENTS</b> .....	<b>53</b>
<b>8 BIBLIOGRAPHY</b> .....	<b>54</b>
<b>9 APPENDIX</b> .....	<b>57</b>
9.1 AERIAL PHOTOGRAPHS OF THE FIELD WORK .....	57
9.2 ORTHOPHOTO OF THE GLACIER.....	65
9.3 ALBEDO MEASUREMENTS .....	65
9.4 MELT MEASUREMENTS .....	67
9.5 RELATIVE DIFFERENCE BETWEEN DURING A STEP CHANGE EXPERIMENT .....	68
9.6 SINUS SIMULATIONS .....	68
9.7 ZONE OF ENHANCED MELT FOR A GLACIER WITH A 20° GLACIER BED GEOMETRY .....	70



---

## List of Figures

Figure 1. Schematic ice-flow diagram for an alpine glacier. (Earle, 2019)	1
Figure 2. Schematic presentation of a debris covered glacier. (Evatt et al. 2015)	2
Figure 3. Yearly mean surface temperature anomalies, Swiss Alpine region in comparison to the global trend. (Haeberli and Beniston, 1998)	4
Figure 4. Østrem curves for different glaciers representing daily rates of ablation with increasing debris thickness. a representing the maximum melt $h_{eff}$ and b representing the debris thickness where melt equals clean ice melt $h_{crit}$ (Nicholson and Benn, 2006)	5
Figure 5. Schematic of a debris glacier system. (Anderson and Anderson, 2016)	8
Figure 6. Figure 1. (a) Geographical location. (b) Zmuttgletscher, its topographical setting and different tributaries. (c) Glacier hypsography in the year 2010 (©SwissTopo); (Mölg et al., 2019).	13
Figure 7. Different surface types: 1st clean-ice surface, 2nd partially covered surface and 3rd fully covered surface	14
Figure 8. Orthophoto of the ablation are of Zmuttgletscher where data was collected during the field campaign, July 2021 (Boris Ouvry)	15
Figure 9. Illustration of step change experiment separated into an (1) initialization phase, where the glacier is building up, (2) a phase where debris is added, (3) a phase where the ELA is increased to a higher elevation and (4) a phase where the ELA is brought back to its previous elevation. In the right plot, a glacier is plotted in each corresponding steady state.	19
Figure 10. Surface changes between first measurements (12.07.2021) and third measurements (5.08.2021). The upper row of images shows the surfaces changes for the fully covered surfaces at location 5D, with an overall increase in larger clasts. The lower three images illustrate the changes that occurred on the partially debris covered surface at location 6D.	22
Figure 11. (a) Relationship between albedo and melt rate for partially debris covered surfaces. (b) aerial view of partially debris covered surfaces with corresponding albedo values with bigger clasts highlighted by red circles, dirt ice with a green area and yellow highlighting debris free areas in images of stake 6D and 7D.	23
Figure 12. Debris thickness change over time. First measurements taken at 12.07.21, second measurements taken at the 5.08.21	24
Figure 13. (a) Østrem curve with varying parameter $D_0$ ; (b) Østrem curve calculated with different equations (FV, C & F1), plotted over collected data during field work on Zmuttgletscher summer 2021	24
Figure 14. Length and volume change after a step change experiment.	31
Figure 15. Length and volume fluctuations following a sinus experiment with a 200-year period.	32
Figure 16. Length and volume fluctuations following a sinus experiment with an 800-year period.	34
Figure 17. Length and volume adjustments to a constantly increasing ELA.	35
Figure 18. Glacier adjustments to a linearly changing ELA.	35
Figure 19. Length and volume adjustments to an ELA forcing representing Swiss Alpine historic climate variations.	36
Figure 20. (a) Debris thickness evolution; (b) debris thickness increase at the beginning of the melt out zone.	37
Figure 21. Zone of enhanced melt rate adjustment to an ELA step change from 3050 m to 3100 m.	38
Figure 22. Zone of enhanced melt rate adjustment to an ELA step change from 3100 m to 3050 m.	39
Figure 23. Length and volume change after a step change experiment (ELA: 3150 → 3200 → 3150 m).	42
Figure 24. Ablation against debris cover. Comparison of (a) results from Fyffe et al., 2020. and (b) results from this study.	45
Figure 25. Adjustment of debris layer to step change experiments. Debris layers are plotted in 10-year steps.	47
Figure 26. Glacier adjustment to a step change of (a) the ELA 3050 → 3100 m in a 50-year step and (b) ELA 3100 → 3050 m.	49

---

<i>Appendix 1. Aerial photographs of each field trip where images were taken of all 16 measurement locations.</i>	64
<i>Appendix 2. Orthophoto of the ablation area of Zmuttgletscher. The red area shows where on the glacier field measurements were conducted as shown in figure 8.</i>	65
<i>Appendix 3. Albedo values at each ablation stake for all three measurements. Differences between the data series are due to weather conditions.</i>	65
<i>Appendix 4. Melt calculations for all 16 stakes.</i>	67
<i>Appendix 5. Relative differences between SMB calculations with enhanced melt vs. no enhancement. Differences in (a) happen in the first 10 years where effects of enhanced melt cause a short period of decline before the debris layer increases in thickness to insulate the glacier.</i>	68
<i>Appendix 6. Sinus simulation with a 400-year period around an ELA of 3050 m with a 50 m amplitude.</i>	68
<i>Appendix 7. Sinus simulation with a 1600-year period around an ELA of 3050 m with a 50 m amplitude.</i>	69
<i>Appendix 8. Adjustment time of the zone of enhanced melt after a step change for a glacier with a 20° sloped bed geometry.</i>	70

## List of Tables

<i>Table 1. Summary of equations used in the modelling experiments to calculate surface melt.</i>	18
<i>Table 2. Important values used for the model parameters standard model (Ferguson and Vieli, 2021).</i>	20
<i>Table 3. Overview of data collected during the field campaign to Zmuttgletscher from 12.07 until 14.09.2021</i>	29
<i>Table 4. Summary of performed modelling experiments.</i>	30
<i>Table 5. Overview of maximal length and volume after different phases.</i>	31
<i>Table 6. Properties of the debris zone with enhanced melt rate after a step change simulation</i>	37
<i>Table 7. Properties of the debris zone with enhanced melt rate after a step change simulation with a slope geometry of 20°</i>	40
<i>Table 8. Properties of the debris zone with enhanced melt rate after a step change simulation with ELA changes of 3150 m → 3200 m → 3150 m</i>	41



---

# 1 Introduction

A glacier is a long-term accumulation of dense ice that moves under its own weight. It forms when snow accumulation exceeds its ablation over many years or millennia. This process can only happen if certain climatic and geographic conditions are met. Glaciers can either be found far North or South where we have low average temperatures due to the interplay between earth's curvature and the sun's incoming radiation, or in regions of high elevation.

Under the strains imposed by its own weight, glaciers slowly deform and flow, forming crevasses, seracs, and other features such as glacier ponds. Additionally, they also build landforms like moraines and fjords by abrading rock and debris from their surrounding landmasses. Glaciers can be identified based on their location (cirque glaciers, expanded-foot glaciers, valley glaciers, niche glaciers, piedmont glaciers), by their basal temperature, which tells us whether or not the glacier has basal movement (warm glaciers) or no basal movement (cold glaciers), or by their function (diffluent glaciers, outlet glaciers) (Mayhew, 2015). A glacier can be divided into two sections: the accumulation area, which adds mass to the glacier, and the ablation area, which subtracts mass from the glacier (Figure 1). The boundary line between these two areas, where no mass change happens, is known as the elevation line altitude (ELA) (Inoue, 1977).

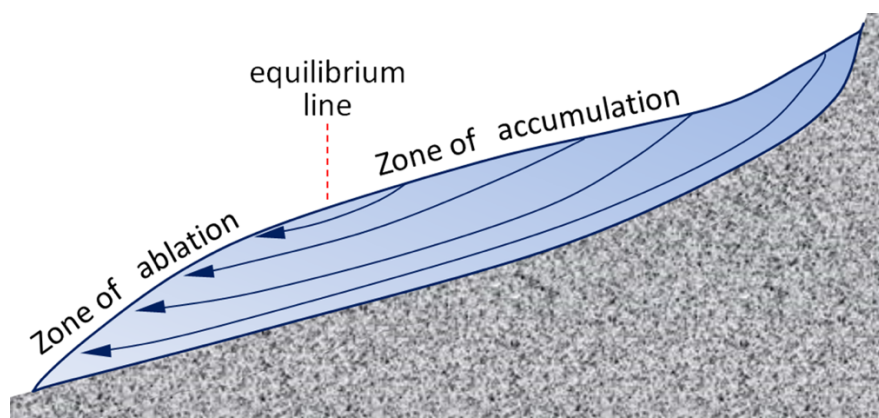


Figure 1. Schematic ice-flow diagram for an alpine glacier. (Earle, 2019)

Debris covered glaciers, a special type of valley glaciers, are a kind of glacier where parts of the ablation area are covered by a continuous cover of debris (Figure 2). On a global scale, excluding the two polar ice sheets, about 4.4 % of all glacier areas are covered by debris, most of which can be found in the Asian Himalaya (Scherler, 2018). Additionally, debris-covered

glaciers can also be found in Peru's Andes, New Zealand's Southern Alps as well as in the Swiss Alps (Nicholson and Benn, 2006). Such glaciers are flanked by steep mountainous headwalls, from which debris breaks off regularly, primarily onto the glacier's accumulation area. From here, debris are incorporated into the ice and transported downstream due to internal movements, resurfacing and accumulating in the ablation area as a result of melt out (Mölg, 2019).

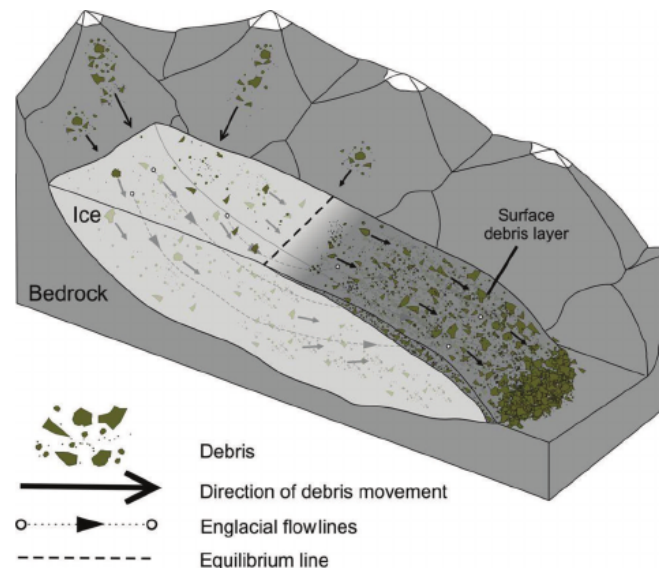


Figure 2. Schematic presentation of a debris covered glacier. (Evatt et al. 2015)

Supraglacial debris has a significant impact on glacier surface mass balance (SMB) because of its insulating effect when debris covers are continuous and thicker than a few centimetres. (Mölg, 2019; Westoby et al., 2020; Ferguson and Vieli, 2021). This effect has also been observed to be a significant factor explaining delayed adjustments of glacier length and volume in response to climate change (Mölg et al., 2019).

In contrast to clean ice melt rates, however, surface melt rates are increased when debris distributions are discontinuous or when layers are thinner than a few centimetres thick. The borderline thickness can differ for each glacier according to local climatic conditions.

In 1959, Østrem established the first empirical relationship between surface melt-rates and supraglacial debris thickness, showing a model with enhanced melt-rates for thin debris layers and an insulating effect for thicker debris layers. (Nicholson and Benn, 2006). The Østrem curve implies that ablation rates increase in comparison to clean-ice for thin layers and decrease for debris cover layer thicker than a certain critical debris thickness, further decreasing with increasing layer thickness. Although these findings have been widely accepted and supported

---

by other independent studies (Loomis, 1970; Mattson et al., 1993; Kayastha et al., 2000), the modelling of debris covered glaciers has yet to incorporate the enhanced melt-rates for thin debris-layers. Most modeling efforts, such as models by Anderson and Anderson (2016), as well as the most recent modeling approach by Ferguson and Vieli (2021), employ a model that does not account for high melt-rates for thin debris layers and instead assumes an insulating effect for all debris layer thicknesses.

Given this information gap for thin debris layers in the modelling of debris covered glaciers, this thesis aims to assess the enhancement effect of thin debris on modeled mass balance and hence glacier evolution. This will be done on the example of Zmuttgletscher (VS) through the following more specific research questions:

- How much does thin debris enhance surface ablation compared to the clean-ice case?
- How can thin debris thickness be quantified and represented in melt models?
- What is the effect of including thin debris in a flow model on the modelled evolution and dynamics of a simplified Zmuttgletscher?

Further research questions that might be covered in the process:

- How long does it take for a thin debris layer with enhanced surface ablation to increase in debris thickness to the point where it has an insulating effect?
- Is the length of the debris zone with increased melt-rate equally long for glaciers with different length?

---

## 2 State of Research

Over the last decades, a vast body of literature on debris-covered glaciers has been published and has increased our understanding of the circumstances required for debris-covered glaciers to exist, as well as the effect debris has on glacial mass balance and melt rates and how climate affects debris covered glaciers differently than clean ice glaciers. A major reason for this increased interest is the global climate change with its far-reaching consequences for the environment and more specifically its effect on glacier retreat rates.

Since the end of the Little Ice Age (LIA) in the 1860's an increase in average temperature can be observed on the whole globe (IPCC, 2021). The effects of climate change are, however, most prominent in alpine regions, where temperature increase is as much as two times as strong as the global trend, as shown in Figure 3 (Haeberli and Beniston, 1998).

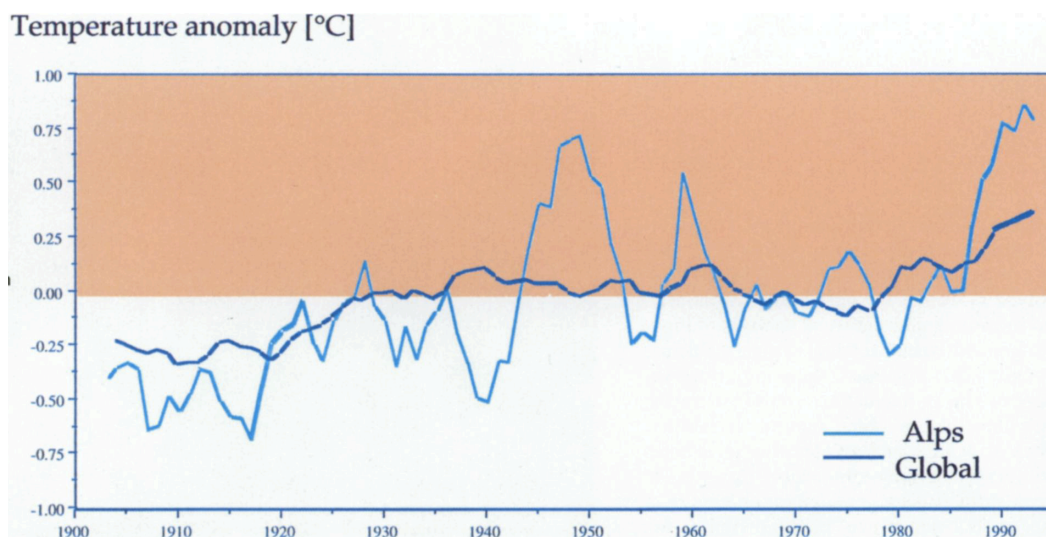


Figure 3. Yearly mean surface temperature anomalies, Swiss Alpine region in comparison to the global trend. (Haeberli and Beniston, 1998)

As glaciers serve as a barometer of climate change, constantly growing or decreasing in response to variations in temperature, the general decline of glacial ice in recent decades has generated worries about water availability, increasing dangers from outburst floods and avalanches, and sea-level change (Benn and Evans, 2010).

In response to this climate influenced glacial recession, a greater attention is also again directed towards debris covered glaciers, as the increasing global temperatures result in an increasing areal coverage of supraglacial debris. For example, Mölg et al. (2019) discovered that since the end of the Little Ice Age (LIA) in 1859, the debris extent on Zmuttletscher, the glacier under research in this thesis, has increased from 13 % to 32 % debris coverage. Similarly, Popovin



and Rozova (2002) calculated a debris cover increase of 8 % from 1968 to 1996 on the Djankuat Glacier in the Caucasus.

The first significant study on debris covered glaciers was established by a publication from Østrem in 1959 where the effects of debris on surface melt rates was first shown and plotted in a curve, henceforward known as the Østrem curve (Figure 4). In his study, Østrem concluded that different ways of energy distribution (outgoing radiation, energy loss to the air by convection and conduction, energy loss through evaporation of meltwater and melting of glacier ice) vary with grain size and thickness of the debris layer. Glacier areas covered by thick debris layers (above 0.5 cm) showed a reduced melt rate in comparison to clean ice, as well as a shorter ablation period. Enhanced melt rate for thin or partially covered surfaces was not measured through ablation measurements but computed using known incoming radiation values. (Østrem, 1959). Despite this, it generated the same results, namely a higher ablation rate in comparison to clean ice (see figure 4, a).

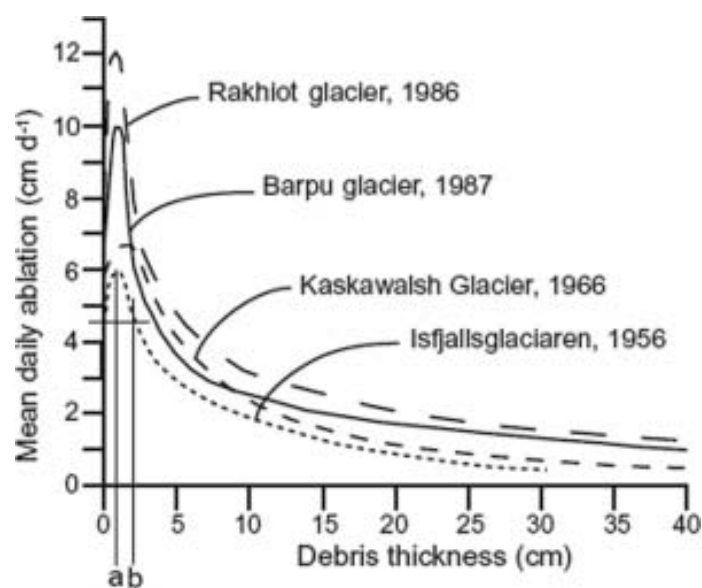


Figure 4. Østrem curves for different glaciers representing daily rates of ablation with increasing debris thickness. *a* representing the maximum melt  $h_{eff}$  and *b* representing the debris thickness where melt equals clean ice melt  $h_{crit}$  (Nicholson and Benn, 2006)

Loomis (1970), as well as Small and Clark (1974), were able to reproduce the “rising limb” of the Østrem curve in their respective studies with an enhanced melt rate of 129 % (Loomis, 1970) and 117.3 % respectively (Small and Clark, 1974). Similarly, a lower melt rate of 78.3 % was found for debris levels of roughly 6 cm, further decreasing with an increasing debris layer thickness (Small and Clark, 1974).



---

To gain a deeper understanding as to why thin debris layers or partially covered layers display higher melt rates, Azzoni et al. (2016) analysed in their study the correlations between ice albedo, debris coverage ratio, and thus, the effects of albedo on surface melt. Albedo represents the fraction of incoming light, which is reflected from a surface, with bright surfaces having a higher reflectance than darker surfaces (Brittanica, 2020). When the critical debris thickness is exceeded, the increased melting rate, due to the lower albedo, is offset by the increased insulation, resulting in an overall decrease in ablation rates. (*Kayastha et al. 2000*; Nicholson and Benn, 2006). The critical debris thickness refers to the debris thickness where the ablation rates for debris covered glaciers and clean-ice glaciers are the same.

For their analysis, Azzoni et al. (2016) set their focus on analysing “fine- and sparse-debris-covered ice and not on actual buried ice” to emphasise the albedo effect on debris coverage ratios (Azzoni et al., pp. 667, 2016). The percentage coverage was calculated using semi-automated image analysis of glacier surfaces. Results of their study showed a high correlation between the debris coverage ratio and ice albedo, with a low debris coverage ratio resulting in a high albedo. With increasing coverage, the albedo decreases. A further finding suggests that the presence of water has a considerable impact on albedo, with results showing a decrease in albedo during the central hours of the day and hence, also higher melt rates. Another observation implies that, during the melt season, albedo decreases over time due to increased surface coverage of fine particles.

Similar studies, such as by Hansen and Nazarenko (2004), concluded that black carbon depositions in the arctic reduced snow albedo by 1-3 % for fresh snow and by an additional factor of 3 as the snow ages, resulting in a significant impact on the climate in recent decades in the Northern Hemisphere (Hansen and Nazarenko, 2004; Azzoni et al., 2016).

Most studies agreed that the critical debris thickness is at most a few centimetres thick only, while Popovin and Rozova (2002) calculated their critical debris thickness to be as high as 7 to 8 cm. It has to be highlighted that these results are found to be in connection with hydrological influenced thawing. The maximum melt rate caused by lower albedo of the debris cover is found for debris layers of about 2cm.

---

As studies have shown a significant correlation between albedo and percentage surface coverage, it is also of importance to quantify how the sub-debris ice ablation is affected by the thickness of the debris layer (Hansen and Nazarenko, 2004; Azzoni et al., 2016; Fyffe et al., 2020). In order to answer this problem, Nicholson and Benn (2006) utilized a generalized numerical model to estimate runoff, calculating sub-debris melt based on daily mean meteorological variables. Unlike Nakawo and Young (1981), who assumed a linear temperature gradient between the upper and lower surfaces of the debris layer with steady state ablation values, Nicholson and Benn used a model that accounted for temperature variability caused by day-time and night-time ablation. Using this model, melt rate beneath debris layer of any thickness can be calculated based on daily mean meteorological data and characteristics of the debris layers (Nicholson and Benn, 2006). Contrary to the results obtained by Østrem and many others (Loomis, 1970; Mattson et al., 1993; Kayastha et al., 2000), Nicholson and Benn's (2006) model suggests no ablation increase for continuous debris layers, independent of their thickness. As soon as the surface is covered by a continuous debris layer, the model predicts decreased ablation. Nicholson and Benn (2006) argue that the 'rising limb' of the Østrem curve can be explained by surface areas that are only partially covered by clots of debris as later confirmed by Fyffe et al., (2020). Predictions for debris layers of several decimetres thickness showed a good fit to actual measurements on their specific study sites.

Due to the substantial variability of empirical approaches for surface mass balance calculations, which are site-specific and highly reliant on the conditions present throughout the measurement periods, generalized numerical models are often preferred. The modelling of valley glaciers is most commonly done with flowline models. In such models, the glacier is modelled as ice moving in a channel defined by the velocity profiles and cross-section-averaged ice thickness (Banerjee and Shankar, 2013). Governed by the laws of physics and based on gathered empirical data, models are now capable of accurately representing real-world circumstances.

One of such model approaches has been brought forward by Anderson and Anderson (2016). Their method uses a two-dimensional valley numerical model that includes englacial and supraglacial debris advection. For the first time, a model that accounts for both boundary conditions at the glacier terminus and variable sources of debris delivery in the accumulation area has been established (Ferguson and Vieli, 2021). Despite knowing about the "rising limb"

of the Østrem curve, for simplicity reasons the enhanced melt rate for thin debris layers has been neglected.

Among other findings, Anderson and Anderson (2016) found that adding debris to a glacier in a steady state while maintaining a constant temperature leads to an almost doubled glacier length. The debris cover has a variety of effects on the glacier, including lowering the mass balance gradient, which is the main reason for the increase in glacier length. The increase in length also results in a reduced ratio of accumulation zone to the total glacier area. The debris cover also affects ice discharge gradients, ice thickness, and surface velocity, all of which are independent of climate change (Anderson and Anderson, 2016).

The researchers discovered that specific delivery paths of debris onto the glacier in the accumulation zone is only of secondary importance to glacier evolution with debris. The crucial factor is the overall debris flux (Anderson and Anderson, 2016).

A more important factor for glacier evolution is where in the accumulation area debris are incorporated. Debris incorporated into the ice near the headwalls result in a debris melt out much further down the glacier, resulting in shorter glaciers with lower fractional debris cover, whereas debris incorporated near the ELA result in an early melt out, resulting in longer glaciers with greater fractional debris cover. This is due to the internal pathways debris takes when being incorporated into the ice as shown in figure 5.

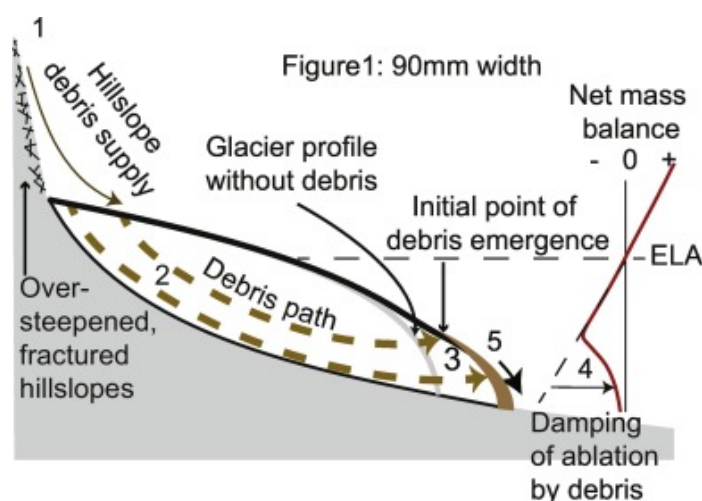


Figure 5. Schematic of a debris-glacier system. (Anderson and Anderson, 2016)

A similar approach to Anderson and Anderson (2016) was published very recently by Ferguson and Vieli (2021), where responses of a debris covered glacier on a simplified geometry have been analysed. For simplicity reasons, similar to Anderson and Anderson (2016), simulations of the enhanced melt zone between debris free and debris covered ice are neglected and an immediate melt reduction with debris cover is used for the modelling approaches performed in

---

this study. The model implies that debris-covered glaciers show an asymmetric response to climate forcing, with a speedy response during expansion but a noticeable lag during retreat. Another interesting finding is that debris-covered glaciers do not have a true steady state, but rather their length is determined by the glacier's history of recurrent cold episodes. A debris-covered glacier that has been subjected to a varying climate forcing and various cold episodes has a longer average length than a debris-covered glacier that has been subjected to a consistent climate forcing, which means that such glaciers are significantly out of sync with the current climate. (Ferguson and Vieli, 2021). Similar to the findings of others (Quincey et al., 2009; Scherler et al., 2011) debris covered glaciers are modelled to experience an almost equally high mass loss as debris free glaciers as the warming has its strongest impact on the upper accumulation area and beginning of ablation area where debris layers are thin. Glacier modelling implies that mass loss happens in two stages, with the first being a relatively quick response in the debris-free zone due to increased melting, followed by a slower response in the debris-covered zone marked by the collapse of the stagnant terminus. However, length fluctuations in response to climate forcing are far more pronounced, as “cold times have a longer-lasting effect on transient length than warm climate periods” (Ferguson and Vieli, 2021). In comparison to a debris free glacier, the model further supports findings of Mölg et al. (2019) that debris thickness and ice flow velocity are linked by an inverse relationship.

A novel approach using a model that involves enhanced melt rates for thin debris layers has been brought forward very recently by Compagno et al. (2021). On the basis of the empirically proven Østrem curve, the model introduces a new formula for calculating melt rates under debris layer below critical debris thickness (the layer thickness where melt rate for debris covered and debris free surfaces are equal). The main goal of the study was to model differences for future scenarios solely based on the differences of including debris cover on Himalayan glaciers or not. Effects of including the “rising limb” of the Østrem curve in comparison to approaches without the “rising limb”, such as made by Anderson and Anderson (2016) or Ferguson and Vieli (2021) were not investigated.

The findings show some extremely interesting conclusions, such as a nearly identical loss of volume for both scenarios, although glacier length vary significantly. Modelled glaciers with debris showed a length reduction of only a few hundred meters (2 % of its length in 2020) whereas debris free glaciers found their steady state to be 20 % shorter than their length in 2020 (Compagno et al, 2021). Similar to the findings of Mölg et al. (2019), an increased debris extent

---

up-glacier is predicted for the modelled glacier. The increased extent of debris is also reflected by an increase in debris layer thickness, which is estimated to increase by about 23 cm for the investigated glacier (Compagno et al. 2021). With a greater area of the glacier being covered by debris as well as covered by thicker layers, the melt rates are expected to decrease. The general higher mass loss, however, still awaits a glacier retreat and down wasting, reducing the debris cover extent. The results, as well as actual data of current state of Himalayan glaciers, show that for the next couple of decades a glacier thinning but no glacier retreat is expected. As Banerjee and Shankar (2013) and others (Quincey et al., 2009; Scherler et al., 2011; Ferguson and Vieli, 2021) already indicated, glaciers identified as stagnant glaciers are still losing volume and a glacial retreat is expected to occur as soon as a maximum debris cover is reached and the debris covered tongue disintegrates (Banerjee and Shankar, 2013; Compagno et al. 2021). Depending on which emission scenario used, the interplay between glacier retreat and increase in debris cover extend vary. Low-emissions scenarios results in an equilibrium towards the end of the century between debris expansion and glacier retreat, whereas high-emission scenarios result in a situation dominated by debris expansion (Compagno et al. 2021).

Despite the fact that Compagno et al. (2021) provided a formula that included enhanced melt rates for thin debris layers, there was no comparison between enhanced melt rates and simulated melt rates with no enhancement to analyse whether or not the enhancement effect has a significant impact on surface mass balance and thus, should be involved in future modelling approaches. Anderson and Anderson (2016) as well as Ferguson and Vieli (2021) both neglected the enhancement effect altogether. Studies that were able to reproduce the “rising limb” of the Østrem curve in their proposed models didn’t evaluate their models based on collected field data but rather “by either varying the proportion of debris cover, or by reducing the evaporative heat flux as the debris thickness” (Fyffe et al., pp. 2273, 2020).

A recent study by Fyffe et al. (2020) put a lot of emphasis on the impacts of thin debris layers. The publication presents a summary table that emphasizes the ambiguity around thin debris layers. Critical debris thickness values collected by multiple studies (Østrem, 1959; Loomis, 1970; Khan, 1989; Mattson et al., 1993; Syverson and Mickelson, 1993; Adhikary et al., 2000; Kayasta et al., 2000; Takeuchi et al., 2000; Konovalov, 2000; Popovin and Rozova, 2002; Hagg et al., 2008; Mihalcea et al., 2008; Brook et al., 2013 and Anderson, 2014) show a high variability, varying for all study sites from only 0.5 cm to as much as 7-8 cm. Furthermore, the

---

enhancement effect varies greatly as well, ranging from an increased melt rate of 117.3 % to 135 % when compared to clean ice. (Fyffe et al., 2020).

The novel approach introduced by Fyffe et al. (2020) uses a high-resolution, spatially continuous ablation map generated by a series of unmanned aerial system surveys as well as on field data collection by means of ablation stakes. Stakes served as ground control points for georeferencing as well as for the validation of the accuracy of the ablation map. In order to be able to use the aerial imagery gathered during a span of two months, the digital elevation models (DEM) had to be repositioned in the XY axis. The percentage coverage of debris was calculated using orthophotos and a point method, where the surface beneath the points was classed as ice or debris (Fyffe et al., 2020).

The findings of this study point to the same conclusion as Nicholson and Benn (2006), namely that the "rising limb" of the Østrem curve can only be explained by partially covered surfaces. Fully covered surfaces of any thickness were found to have a lower ablation. Furthermore, clean ice is difficult to find and as the study indicates, a so-called clean ice surface needs to have less than 15 % debris cover in order to have a lower ablation rate as other partially covered surfaces. In comparison to debris-free ice, ablation was found to be up to 20 % higher on partially covered surfaces. For the partially debris covered surfaces, Fyffe et al. (2020) found an inverse relationship between albedo and ablation. With an increase in percentage debris cover, the albedo decreases, and the ablation rate increases.

Further, ablation rates for partially debris-covered surfaces ranging from 30 to 80 % coverage were found to be relatively similar. This is thought to be related to the fact that albedo and clast size have opposing roles. While an increase in percentage debris cover decreases the albedo, resulting in a higher intake of net shortwave radiation, the same effect also causes a melt out of larger clast sizes, resulting in less ablation due to their increased thickness. (Fyffe et al., 2020). The findings of this study also show that obtaining the "raising limb" with field data is challenging and can only be attributed to partially covered debris layers.

Even though Zmuttgletscher cannot be directly compared to high mountain Himalayan debris covered glaciers, being of much smaller extent and being influenced by a different environment, the study of Mölg et al. (2019) is of particular interest here, as field measurements of this thesis are carried out on Zmuttgletscher. And despite being a much smaller glacier, findings, such as the expansion of the debris up-glacier, as was found by Mölg et al. (2019) is a common response of glaciers to increased global temperatures and is also observed for

---

glaciers in the Himalayas, the Peru's Andes or the New Zealand's Southern Alps. At Zmuttgletscher, similar to many other studies, ablation measurements for increased debris thickness also follow the Østrem curve. As Zmuttgletscher does not have a homogenous distribution of debris cover, it is possible to find different debris thickness levels and varying melt rates on roughly the same elevation, which allows the conclusion that melt is much rather dependent on debris thickness than elevation (Mölg et al. 2019). Additionally, findings from Zmuttgletscher conclude that the increased extent of debris is a result of two factors: elevated temperatures as well as a decreased flow velocity of the ice. The reason for this assumption is the rather small glacier size (and thickness) which results in a shorter response time. Nevertheless, in comparison to debris-free glaciers, debris covered glaciers, such as Zmuttgletscher, have been observed to show a delayed reaction to climatic changes. A further finding in this regard suggests that glacier thinning for debris covered glaciers is independent of elevation for lower elevation areas. In contrast at the case for debris free glaciers, melt is generally observed to increase towards the terminus. This non-linearity for debris covered glaciers results in more extended glacier tongues. Despite these findings, the data show that climatic forces still dominate the evolution of Zmuttgletscher, as the overall debris layer is relatively thin but still sufficient to prevent glacier thinning and terminus retreat.

### 3 Methodology

#### 3.1 Study Area

Zmuttgletscher is a valley glacier located in the southern end of the Matter Valley in the western Swiss Alps with a ~2239 to 4030 m elevation range. It has a surface area of about 15 km<sup>2</sup> and a length of 7.9 km, which makes Zmuttgletscher a medium-sized Alpine glacier (©SwissTopo). Zmuttgletscher is surrounded by the Dent d' Herens and the Matterhorn to the south, by the Tete Blanche to the west and by the Dent Blanche to the north. The high rock walls around its accumulation basins, with elevation differences of up to 1500 meters, provide debris into the glacial system, resulting in a heavily debris-covered ablation area. As a result, around 32.7 percent of Zmuttgletscher is debris covered (Mölg et al., 2019). The Zmuttgletscher accumulation area has its tributary glaciers Schönbielgletscher to the north, Stockjigletscher to the west, and Tiefmattengletscher to the south (see figure 6). Nowadays, the main tributary is the Tiefmattengletscher to the south.

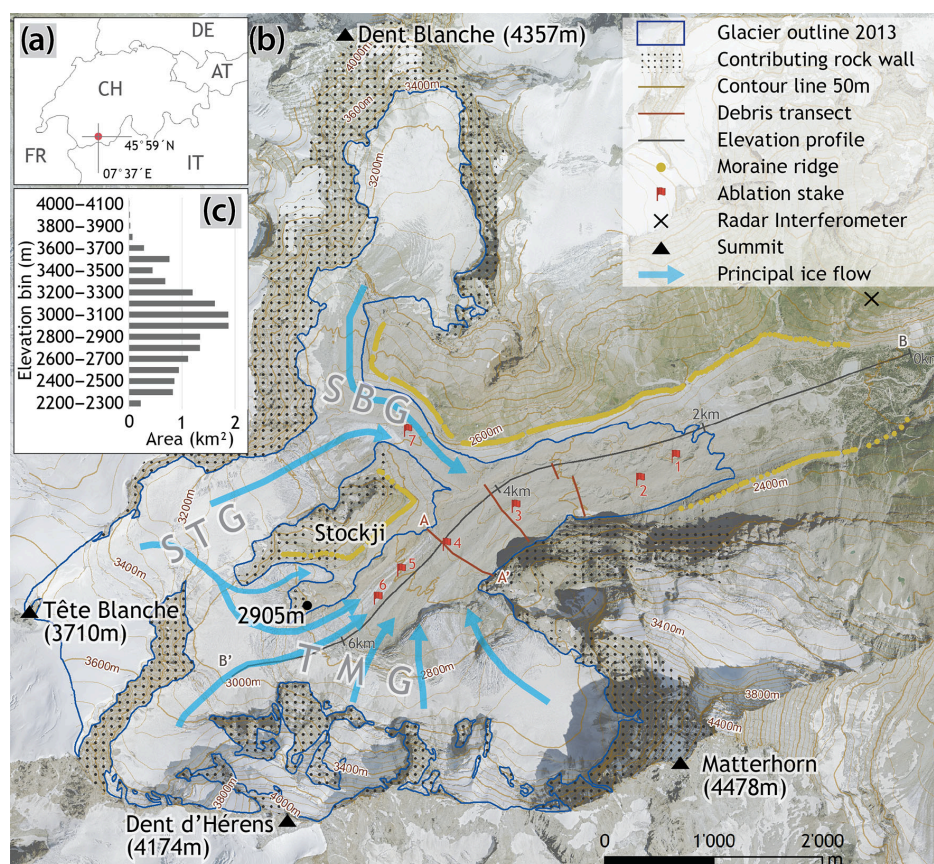


Figure 6. Figure 1. (a) Geographical location. (b) Zmuttgletscher, its topographical setting and different tributaries. (c) Glacier hypsography in the year 2010 (©SwissTopo); (Mölg et al., 2019).

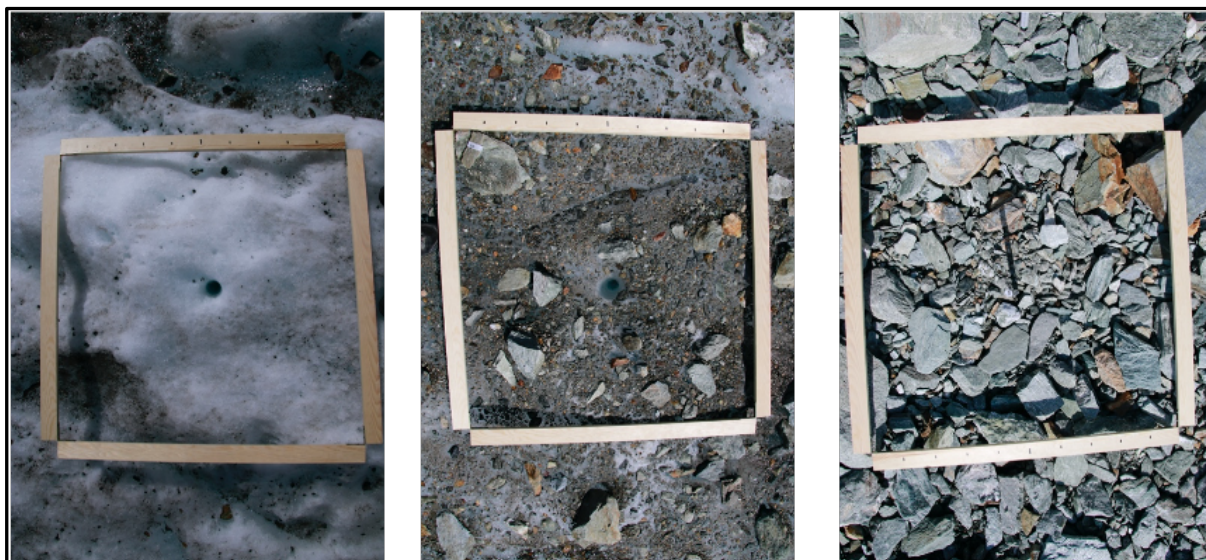


---

## 3.2 Field Measurements

Measurements were taken during a field campaign to Zmuttgletscher in Zermatt (VS), lasting from the 12<sup>th</sup> of July until the 23<sup>rd</sup> of September 2021. A total of four field visits to the Zmuttgletscher were scheduled during this time period. In order to reduce variability in temperature at each site, all measurements were conducted in the top part of the ablation area of the Zmuttgletscher at an elevation of roughly 2600 meters above sea level (see Appendix A2). To further limit variability, locations of comparable slope gradients were chosen. The ablation measurements were performed by means of white plastic ablation stakes.

During the first field trip, a total of 14 stakes were drilled into the ice with varying levels of debris thickness (0 – 19 cm). For reference values, two stakes were drilled into debris-free areas. All stakes were marked accordingly for later processing of the data. Figure 6 shows the encountered surface types where ablation stakes were drilled into: clean ice, partially covered and fully covered. Clean ice surfaces are not 100 % debris free however, as can be seen on the first image in figure 7.



*Figure 7. Different surface types: 1st clean-ice surface, 2nd partially covered surface and 3rd fully covered surface*

The orthophotos, along with albedo values, were used to analyse the partially covered glacier surfaces.

During the second field trip, two more stakes were installed to offer extra data points for thin debris layers. Figure 8 gives an insight into where the measurements were taken. To get a better

idea on where on the glacier the measurements were performed, an orthophoto of the entire ablation area of the glacier can be found in Appendix A2.

At each location, the following information were measured: incoming shortwave radiation and outgoing shortwave radiation with an albedometer for the calculation of albedo, slope angle and aspect angle to make sure that all analysed locations have similar angles, debris thickness, geographic coordinates and heights above sea-level with a simple GPS, images with an aerial viewpoint, and ablation. For the images, a canon EOS760D with a Tamron 18-200 mm lens was used to capture the surface by a 1x1 m grid. The dimension 1x1 m was chosen based on a similar dimension used by Azzoni et al. (2016). A total of five debris thickness measurements and four ablation measurements were conducted each time.

During the second to fourth field trip, only albedo, images with aerial perspective and ablation were taken. Additionally, debris thickness was measured again on the third trip to Zmutt glacier.

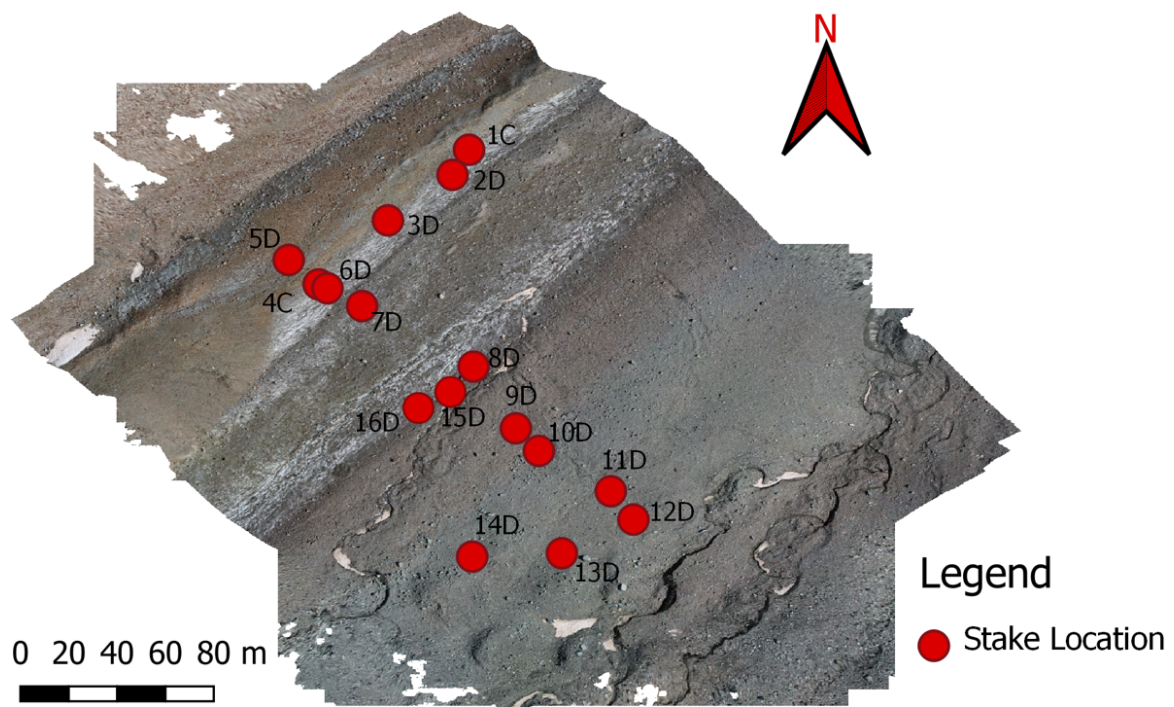


Figure 8. Orthophoto of the ablation are of Zmuttletscher where data was collected during the field campaign, July 2021 (Boris Ouwry)

---

### 3.3 Modelling

For the modelling part the numerical model from Ferguson and Vieli (2021) was used. In this part, only the most important aspects in regard to the thesis will be mentioned. For a more in-depth explanation of all facets of the model utilized in this thesis, refer to Ferguson and Vieli (2021).

The DEBISO model includes an ice flow model and a debris transport model, with the debris transport model including debris melt-out and its insulating effect on ice ablation (Ferguson and Vieli, 2021). As a result of the inclusion of the debris transport, the geometry and ice flow are affected by changes in the surface mass balance. Additionally, the cryokarst effects are also accounted for in the model, although so far rather crudely. Cryokarst are erosional structures (pits and depressions) thought to be generated by sublimation-driven subsurface ice loss and subsequent surface collapse (Kreslavsky et al., 2008). For the investigations conducted in this thesis however, the effects of cryokarst on SMB are neglected.

For the modelling of the ice flow, the shallow ice approximation (SIA) has been used. The SIA disregards the additional components and equations for a realistic and qualitative modelling of glaciers due to its use of the shallow ice ratio (ratio of vertical to horizontal characteristic dimensions) (le Meur et al., 2004). As a result, the complexity of model equations and boundaries is greatly reduced.

For the debris distribution, the model assumes that the debris is equally distributed across the glacier, homogeneous in size, and has a constant concentration within the ice. A debris concentration of 0.25 percent was utilised for all calculations as a default value based on the study of Ferguson and Vieli (2021). As a result, ice melt steadily adds debris to the surface source in the ablation area and creates a debris layer increasing in thickness the further down we go along the ablation zone. Debris is moved downhill when it has melted out, until it reaches the terminus. It is important to note that this model is representative of heavily debris-covered glaciers with debris deposition in the accumulation area close to or even beyond into the ablation area (Ferguson and Vieli, 2021). As a result of this, the entire ablation area is covered in debris.

---

Surface mass balance is calculated as an elevation-dependent function. In the original model by Ferguson and Vieli (2021), mass balance for the debris covered glaciers are calculated by

$$(1) \quad a = a_H * \frac{D_0}{D_0+D}$$

where  $a$  is the calculated mass balance,  $a_H$  is the elevation-dependent mass balance for debris free surface mass balance (SMB),  $D$  is the debris thickness and  $D_0$  is a free parameter that is chosen so that it exhibits the best Østrem curve for the data obtained in the field. The value used for  $D_0$  is determined by the Østrem curve that represents the glacier under consideration. Enhanced melt rates for  $D < D_0$  are neglected in this equation.

To include the enhanced melt rates for debris thicknesses below the threshold debris thickness ( $D_0$ ), two different relationships between debris thickness and surfaces mass balance are used. For the first version, the equation (2) postulated by Compagno et al. (2021) was implemented into the numerical model. Here, SMB is calculated as follows:

$$(2) \quad \begin{aligned} a &= a_H * \frac{D_0+h_{crit}}{D_0+D} && \text{if } D > h_{crit} \\ a &= a_H * \left( \frac{D_0+h_{crit}}{h_{eff}+D_0} * \frac{D}{h_{eff}} + \frac{h_{eff}-D}{h_{eff}} \right), && \text{if } D < h_{crit} \end{aligned}$$

with  $h_{crit}$  representing the critical debris thickness, where the melt rate equals the melt rate of debris free surfaces and  $h_{eff}$  representing the debris thickness where melt is maximal.  $a$ ,  $a_H$ ,  $D$  and  $D_0$  are the same as in the equation (1).

The second relationship (equation 3) uses a constant enhancement factor  $f_{enh}$  for melt debris thickness below the threshold  $h_{crit}$  and for debris layers greater than  $h_{crit}$  are calculated based on equation (1) by Ferguson and Vieli (2021). Two different melt enhancement factors  $f_{enh}$  of 1.2 and 1.6 are explored (see table 1).

A first melt enhancement factor  $f_{enh}$  is derived from the data collected during the Zmuttgletscher field campaign, where the melt rate was found to be 1.2 times higher than the clean ice melt rate. The higher value used for the enhancement factor of 1.6 is based on an averaged effective multiplier of melt rates of multiple debris covered glaciers as used in Compagno et al. (2021).

$$(3) \quad \begin{aligned} a &= a_H * \frac{D_0}{D_0+D} && \text{if } D > h_{crit} \\ a &= a_H * f_{enh} && \text{if } D < h_{crit} \end{aligned}$$

Table 1. Summary of equations used in the modelling experiments to calculate surface melt.

Number	Equation	Referenced as	Abbreviation
(1)	$a = a_H * \frac{D_0}{D_0 + D}$	Ferguson and Vieli (2021)	FV*
(2)	$a = a_H * \frac{D_0}{D_0 + D}$ $a = a_H * + \frac{D_0 + h_{crit}}{h_{eff} + D_0} * \frac{D}{h_{eff}} + \frac{h_{eff} - D}{h_{eff}}$ ,	if $D > h_{crit}$ if $D < h_{crit}$ Compagno et al. (2021)	C*
(3.1)	$a = a_H * \frac{D_0}{D_0 + D}$ $a = a_H * 1.2$ ,	if $D > h_{crit}$ if $D < h_{crit}$ Farsky1.2	F1*
(3.2)	$a = a_H * \frac{D_0}{D_0 + D}$ $a = a_H * 1.6$ ,	if $D > h_{crit}$ if $D < h_{crit}$ Farsky1.6	F2*

\*Equations will from now on be referred to by their abbreviations.

To compare the behaviour of the glacier in response to the three different debris-effect equations, glacier evolution was simulated for a range of climate forcing experiments as listed below, and in which temperature variations are represented by changes in the level of the ELA:

- a) A step change simulation, where the ELA is set to a higher elevation for 2000 years to reach a steady state and later returned to the previous elevation to reach a steady state once more (3050 → 3100 → 3050 m.a.s.l.)
- b) Sinus simulations around a set ELA of 3050 m with an amplitude of 50 m. Four different time periods were used (200, 400, 800 & 1600 y period).
- c) A gradual increase of the ELA with a linear increase of the ELA of 120 m per 100 years, which is representable of the ELA increase in the Swiss Alps in the last 100 years (Casty et al., 2005).
- d) A variable ELA forcing time series, calculated by Lüthi et al. (2010) and which depicts the ELA's history in the Swiss Alps from using a volume change reconstruction based on length change data from Swiss glaciers.

In general, a complete model run is separated in three to four phases. In the initialization part a clean ice glacier is built up under a constant ELA until reaching a steady state. The second phase involves adding debris to the ablation area while keeping the ELA at the same elevation. This phase lasts until the glacier establishes a steady state once more. For all experiments conducted, these initialization phases remain unchanged. In the third phase the actual climate change experiments are conducted, where the ELA is for (a) behaving in a sinusoidal manner



around the previous elevation of the ELA, for (b) is increased to a higher elevation, for (c) is gradually increasing and for (d) is following a temperature forcing representing the past climate in the Swiss Alps. A fourth phase is only implemented in the step change experiment to take the ELA back to the previous elevation.

To further analyse the variations in the length of the debris layer zone with enhanced melt rates, which is here defined as the area in the ablation zone where the debris thickness ranges from  $< 0\text{m}$  to  $0.03\text{m}$ , two further experiments are conducted:

- e) Change of the bed geometry, where the slope of the linear bed is increased to  $20^\circ$
- f) Step change experiment with a constant ELA of  $3100\text{m}$  for the build-up phases and changes to  $3150$  and back to  $3100\text{m}$  in the third and fourth phase of the model run

All other experiments (a, b, c and d) have a simplified bed geometry consisting of a default short steep headwall with a slope of  $45^\circ$  followed by a linear bed with a slope of around  $10^\circ$  (Ferguson and Vieli, 2021).

In a last experiment (g) the free parameter  $D_0$  is increased from  $0.05$  to  $0.1$  and a simple step change simulation is performed as illustrated in figure 9.

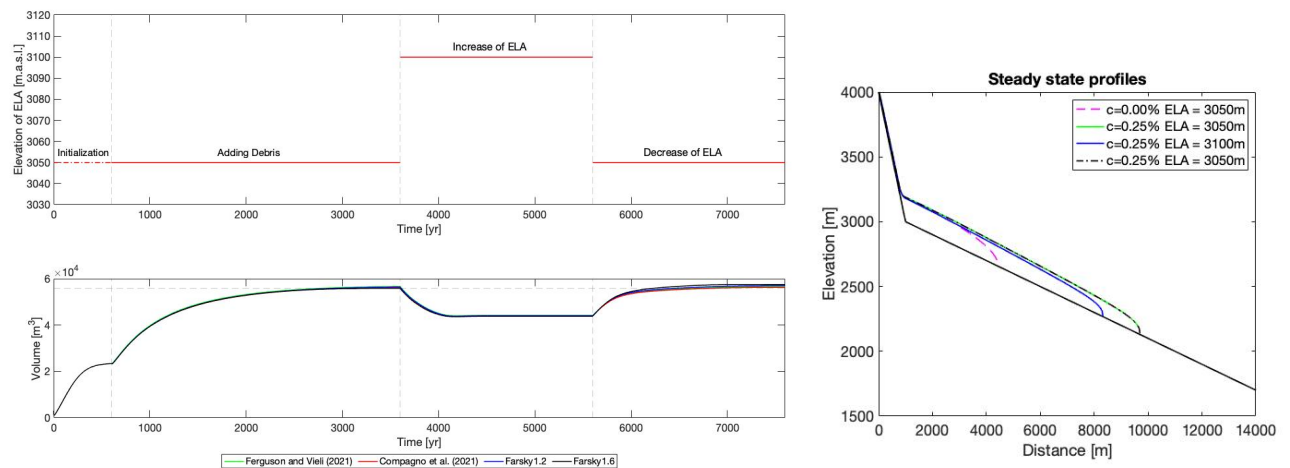


Figure 9. Illustration of step change experiment separated into an (1) initialization phase, where the glacier is building up, (2) a phase where debris is added, (3) a phase where the ELA is increased to a higher elevation and (4) a phase where the ELA is brought back to its previous elevation. In the right plot, a glacier is plotted in each corresponding steady state.

Table 2. Important values used for the model parameters standard model (Ferguson and Vieli, 2021).

Parameter	Name	Value	Unit
ELA	Elevation Line Altitude	3050	m.a.s.l
$\rho$	Density of ice	910	kg m <sup>-3</sup>
g	Gravitational acceleration	9.80	m s <sup>-2</sup>
c	Debris volume concentration	0-0.005	%
A	Flow law parameter	1 x 10 <sup>-24</sup>	Pa <sup>-3</sup> s <sup>-1</sup>
n	Glen's constant	3	
D <sub>0</sub>	Characteristic debris thickness	0.05/0.1	m
a <sub>max</sub>	Maximum surface mass balance	2	m yr <sup>-1</sup>
$\gamma$	Surface mass balance gradient	0.007	yr <sup>-1</sup>
H*	Terminal ice thickness threshold	30	m
dt	Time step	0.01	yr
dx	Spatial discretization	25	m
$\theta$	Bed slope	0.1	m m <sup>-1</sup>
$\theta_c$	Headwall slope	1	m m <sup>-1</sup>
Sinus Simulation			
a	Amplitude	50	m
T	Period	200/400/800/1600	yr
Step Change			
ELA	Elevation Line Altitude	3050 → 3100 → 3050	m.a.s.l
Gradual Increase			
grad	ELA increase	0.8	m/yr

Differences in response to the use of different equations for SMB calculations will be illustrated by comparisons of volume and length of the glacier, as well as by comparisons of the debris thickness differences along the ablation zone.

---

## 4 Results

### 4.1 Field Measurements

#### 4.1.1 Image analysis

During three of the four visits to Zmuttgletscher, aerial images were taken of all measurement locations. Three surface types were analysed: clean ice surfaces, partially covered surfaces and debris covered surfaces. It must be emphasized that the clean ice surfaces are not completely clean. As shown in figure 6, part of the 1x1 m square clean ice can be classified as dirt ice. Furthermore, the partially covered surfaces with a low percentage coverage are almost only dirt ice with an increase in on-surface clasts resulting in an increase in percentage coverage.

The aerial images reveal surface changes for the partially covered surfaces with higher percentage coverage as well as for one of the fully covered surfaces (5D). The other fully covered surfaces only show small changes in debris arrangement (see figure A1).

The upper images of figure 10 show the images taken for stake 5D. The image taken after installing the ablation stake on the 12.07.2021 (left) still shows areas of clast sizes of <1 cm as well as sandy-dirt areas, and not too many bigger clasts, whereas the image taken on the 8.08.2021 (right) shows a significant increase in bigger clasts, which is indicative of vigorous surface movements.

The lower images of figure 10 show the partially covered surfaces of stake 6D. An example of a surface change can be seen in the upper right-hand side of the image obtained on the 12.07.2021. It displays a nearly debris-free surface, whereas the same area in the image taken on the 8.05.2021 is now covered by debris. The most salient change, however, is the occurrence of a big clast in the last obtained image. Similar changes can be observed for the other surface of higher percentage coverage (figure A1).





Figure 10. Surface changes between first measurements (12.07.2021) and third measurements (5.08.2021). The upper row of images shows the surface changes for the fully covered surfaces at location 5D, with an overall increase in larger clasts. The lower three images illustrate the changes that occurred on the partially debris covered surface at location 6D.

#### 4.1.2 Debris coverage and albedo

As results indicate, albedo decreases with an increase in debris coverage in comparison to clean ice surfaces (see figure 11b). For fully covered surfaces, albedo solely depends on lithology and not on layer thickness. Albedo measurements were taken three times, each time under different weather conditions and at different times of the day, resulting in day-to-day variation (see Appendix A3).

The averaged ice albedo measured by the mobile net radiometer varied from 0.112 to 0.293, with clean ice albedo ranging between 0.245 and 0.293, fully debris covered albedo between 0.112 and 0.164 and partially debris covered surfaces between 0.116 and 0.204.

The correlation between albedo and debris cover is best shown in figure 11a, where albedo is plotted against melt rate of percentage debris covered surfaces as well as for the clean ice surfaces. With an increase in percentage debris cover, the albedo decreases. The average clean ice melt rate of the two stakes is at 5.3 cm/d with an average albedo of 0.27. With an increase in debris percentage coverage, the albedo decreases by a factor of -0.1189.

No specific calculations were performed to precisely calculate the percentage coverage of the partially covered surfaces but based on visual inspection, the percentage coverage increases the following:  $2D < 3D < 6D < 7D$ . Figure 11b illustrates the four partially covered surfaces with highlighted areas responsible for a decrease in albedo.

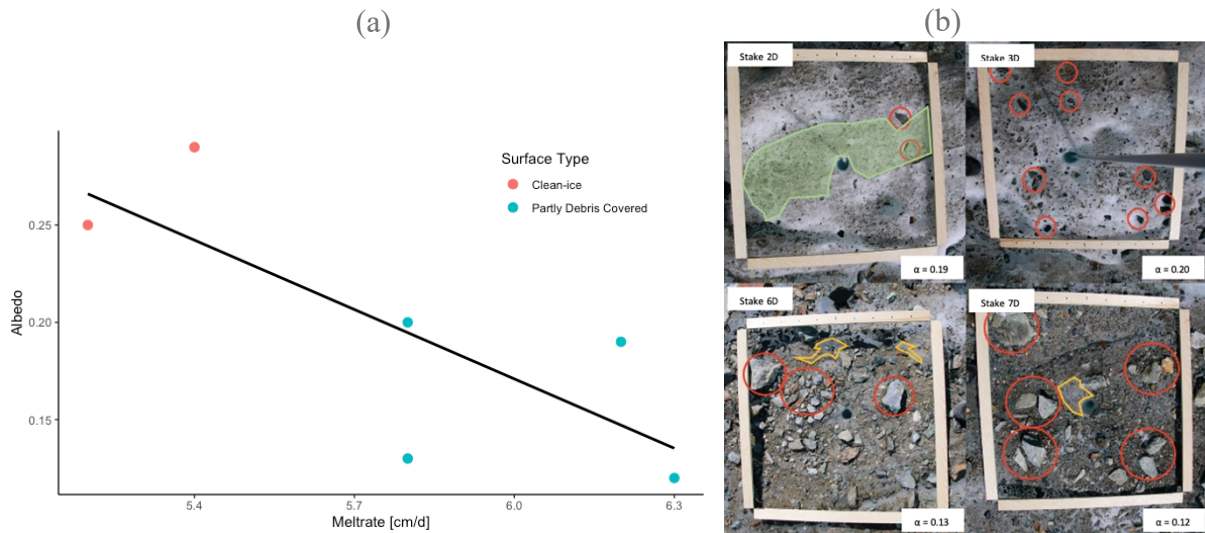


Figure 11. (a) Relationship between albedo and melt rate for partially debris covered surfaces. (b) aerial view of partially debris covered surfaces with corresponding albedo values with bigger clasts highlighted by red circles, dirt ice with a green area and yellow highlighting debris free areas in images of stake 6D and 7D.

Debris thickness was measured twice at each location. Changes were observed for all stakes, although with the exception of stakes 13D and 5D, all differences were within a 2 cm error range, which is considered a reasonable range for measurement error. (see figure 12). The minimum measured continuous layer of debris was measured at 0.7 cm at stake 5D. At this location the debris thickness increased to an average of 3.1 cm during a time period of 25 days. This increase in debris thickness is to some extent also visible in the images, where an overall increase in clast size has been observed (figure 10). The thickest layer on which measurements were taken was 19.2 cm thick. A second measurements 25 days later at stake 13D showed a reduction in layer thickness to only 11.4 cm.

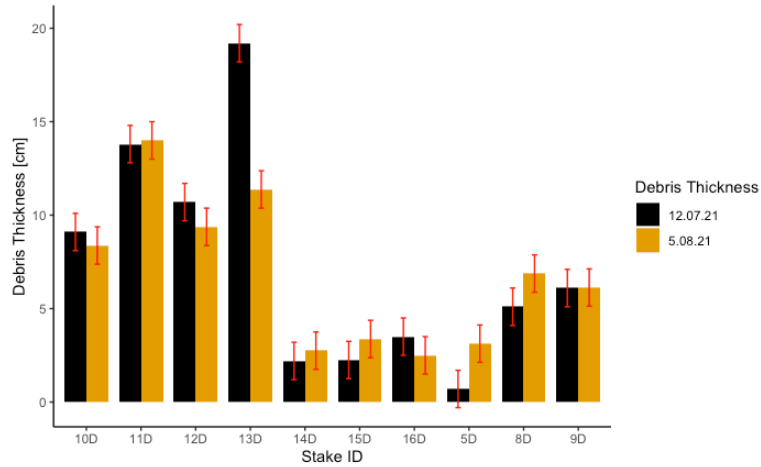


Figure 12. Debris thickness change over time. First measurements taken at 12.07.21, second measurements taken at the 5.08.21

### 4.1.3 Ablation Measurements

Melt rates collected during the field campaign agree with the Østrem curve as shown in figure 13. The averaged melt rate per day of the clean ice surfaces is measured at 5,3 cm/day. All four partially debris covered surfaces have a higher melt rate and the fully covered surfaces decrease in melt rate with increasing debris thickness as shown in figure 13. The maximum melt rate  $h_{eff}$ , measured at stake 7D, the partially covered surface with the highest percentage coverage, is found at 6.35 cm/day, which is an increase by a factor of 1.2 to clean ice. The lowest melt rate measured beneath a debris surface is 2.06 cm/day, which is a reduction of 62 % in comparison to the clean ice melt. All fully covered surfaces have a decreased melt rate in comparison to the melt rate of clean ice, decreasing with an increase in layer thickness.

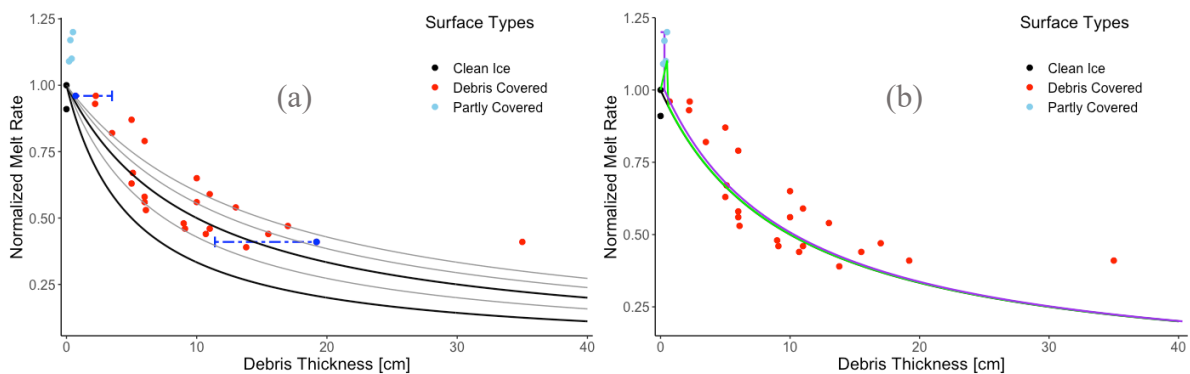


Figure 13. (a) Østrem curve with varying parameter  $D_0$ ; (b) Østrem curve calculated with different equations (FV, C & F1), plotted over collected data during field work on Zmuttgletscher summer 2021

---

As shown in figure 13a, the slope of the curve representing an Østrem curve without the rising limb is calculated based on the formula

$$a = a_H * \frac{D_0}{D_0 + D}$$

which has also been used for the numerical modelling by Ferguson and Vieli (2021). The decrease in melt rate with an increase in debris thickness is based on the adjustable parameter  $D_0$ .  $D_0$  describes how the slope behaves with increased debris thickness. Values of 0.05, 0.075, 0.1, 0.125 and 0.15 m for  $D_0$  are plotted in figure 13a overlain to the point measurements collected from Zmuttgletscher. The best fit for the empirically collected data is a value of  $D_0 = 0.1$  m. For the modelling approaches the parameter  $D_0$  has been given the value of 0.05 m however, as it was used in the study from Ferguson and Vieli (2021).

In figure 13a stakes 5D and 13D are highlighted and their possible range of debris thickness marked with an error range. Especially at 5D ablation rates have changed significantly with an increase from 0.7 cm to 3.1 cm.

Three equations are used for the numerical model, all of which are plotted in figure 13b with  $D_0 = 0.1$  m. Significant differences are only visible in the first 3 cm's with two equations having the enhancement implemented.

A general overview on the information acquired during the field campaign is summarized in Table 2. More precise descriptions of the collected data can be found in the Appendix A4.

Table 3. Overview of data collected during the field campaign to Zmuttgletscher from 12.07 until 14.09.2021

Stake ID	slope angle [°]	aspect angle [°]	Elevation [masl]	Debris thickness [cm]	Albedo	Total melt [cm]	Average melt per day [cm/d]
1C	-3	42	2599	NA	0,245	126	5,2
2D	-5	42	2599	NA	0,191	149,75	6,19
3D	-8	42	2600	NA	0,204	139,5	5,76
4C	-2	42	2612	NA	0,293	130,625	5,4
5D	-8	102	2611	0,7	0,142	122,5	5,07
6D	-4	32	2611	NA	0,125	141,25	5,84
7D	-9	79	2610	NA	0,116	153,375	6,35
8D	-7	28	2618	5,1	0,151	86,25	3,57
9D	-4	328	2618	6,1	0,153	67,375	2,79
10D	-3	52	2615	9,1	0,164	58,625	2,43
11D	-8	42	2614	13,8	0,161	49,75	2,06
12D	-6	28	2622	10,7	0,155	55,75	2,31
13D	15	238	2623	19,2	0,163	51,875	2,15
14D	-12	335	2612	2,2	0,126	118,75	4,95
15D	-13	305	2609	2,25	0,112	76,7	5,09
16D	-7	355	2613	3,5	0,131	65,6	4,36

C = clean ice, D = debris covered



---

## 4.2 Modelling

To understand whether or not the inclusion of enhanced melt for thin debris layers is important, results of conducted numerical experiments will be shown in this part. A summary of the modelling experiments that were carried out can be seen in Table 4.

*Table 4. Summary of performed modelling experiments.*

Experiment	Description	Section	Figures
a	Step change with steady states at ELA = 3050,3100,3050 m	4.2.1	14
b	Sinus simulation	4.2.2	15, 16
c	Gradual increase of the ELA	4.2.3	17
d	ELA forcing	4.2.4	18
e	Step change with a steeper slope of 20°	4.2.5	-
f	Step change with steady states at ELA = 310,3150,3100 m	4.2.6	-
g	Step change with different $D_0$ of $D_0=0.1$	4.2.7	22

### 4.2.1 Step Change Simulation

A step change simulation is one approach to compare reaction time and adaption time of volume and length for the four different equations for surface mass balance (SMB) calculation used in this study as shown in figure 14. The effect of the enhanced melt rate can be seen in the plots a1 and a2 already where all three simulated glaciers with enhanced melt have a slight reduction in volume and length. A steady state is reached first by a SMB calculated by equation F2. Taking a closer look at the curves of all four equations, it can be seen that the differentiation happens at the very beginning when debris is added to the glacier. The curve depicting a glacier without enhanced melt increases as soon as debris is added, whereas the other three curves all have a short decrease in volume, before the effects of insulation cause an increase in volume (see figure 14). Afterwards, the increase is similar between all four approaches (see Appendix A5).

Exact values for all phases of the simulation are provided in table 5. In the plots b1 and b2 the response of all glaciers to a sudden change of the ELA from 3050 m to 3100 m can be seen. The volume of all glaciers decreases as soon as the ELA is moved to the higher elevation, whereas the glacier length needs about 180 years to respond to the change in ELA when SMB is calculated with equations FV, C or F1. Only F2, where the melt enhancement is greatest, has a quicker reaction time of 129 years. A steady state is reached for all glaciers within 600 to 630 years. An interesting observation here are the volume changes. The debris covered glaciers

overshoot their true steady state volume about 550 to 600 years after the step change. After reaching this state, the volume increases slightly again the following 500 years without changing the length of the glacier. The third phase of the experiment is shown in plots c1 and c2, where an instant increase in volume and length can be observed in response to the lowering of the ELA to 3050 m. Glaciers where SMB is governed by equations FV and C reach almost the exact steady state length and volume as they have done at the end of phase 2. Interestingly however, F1 and F2 reach a steady state with an increase in volume and length and are thus, greater in length and volume as a FV glacier. Despite these findings, F2 still reaches its steady state earliest about 300 years earlier than the other three simulations.

The overall behaviour to a step change of the ELA is similar for all four equations with F2 having the quickest reaction and adaption time.

Table 5. Overview of maximal length and volume after different phases.

	Ferguson (2021)	Compagno (2021)	Farsky1.2	Farsky1.6
Adding debris	l = 9'700	l = 9'675	l = 9'675	l = 9'575
	v = 56'679	v = 56'263	v = 56'440	v = 55'852
ELA increase to 3100 m	l = 8'325	l = 8'300	l = 8'325	l = 8'275
	v = 44'194	v = 43'918	v = 44'076	v = 43'805
ELA decrease to 3050 m	l = 9'700	l = 9'675	l = 9'750	l = 9'775
	v = 56'694	v = 56'265	v = 57'045	v = 57'353

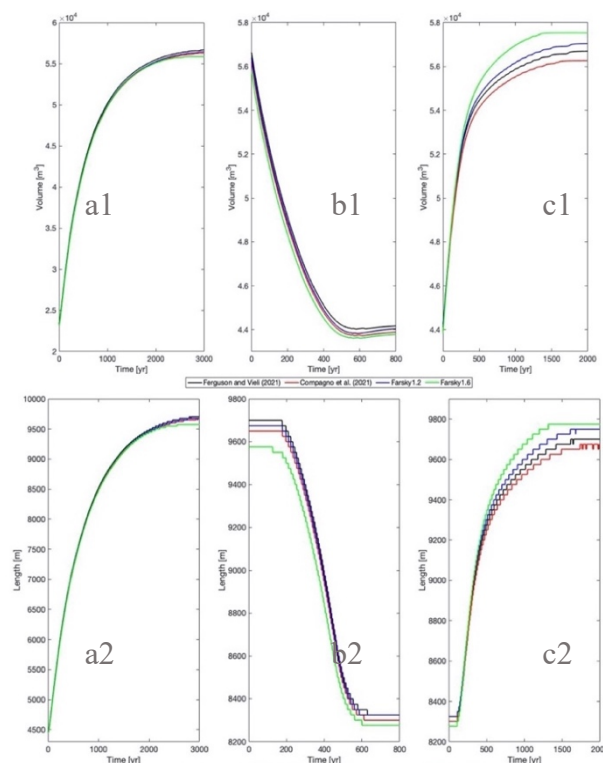


Figure 14. Length and volume change after a step change experiment.

## 4.2.2 Sinus Simulation

The purpose of the sinus simulation studies is to evaluate the reaction time to changes in the ELA of debris-covered glaciers throughout various sinus periods. A further comparison to a clean ice glacier is additionally performed for a 200- and 800-year period.

The starting conditions for all presented experiments in this segment are the same as shown in figure 14, plots a1/a2. An important point to mention is that a lowering of the ELA equals a decrease in temperature and thus, results in an increase in volume and length of a glacier. An increase of the ELA to a higher elevation thus, results in a glacier retreat.

Over a 200-year sinus period, volume for all equations, as well as for a clean ice case, show a sinusoidal behaviour with a shift of around 50 years relative to the sinus behaviour of the ELA (see figure 15). Reaction times to a minimum of the ELA are slightly shorter than to a maximum for the debris covered glaciers (~48 yr vs ~51 yr). Differences between maximum and minimum are significantly smaller for debris covered glaciers, with an average volume difference of 3'763 m<sup>3</sup>. The volume difference for the clean ice case is found at 7'979 m<sup>3</sup>.

Length variations for debris covered glaciers in response to the sinus fluctuations cannot be identified under a 200-year period. Taking a closer look at the progression of the curve however, a constant increase is discernible. The clean ice glacier on the other hand exhibits a sinusoidal behaviour for its length, although it's less refined than the volume fluctuations. Maximums and minimum in length are reached 10-15 years later than the corresponding volume peaks.

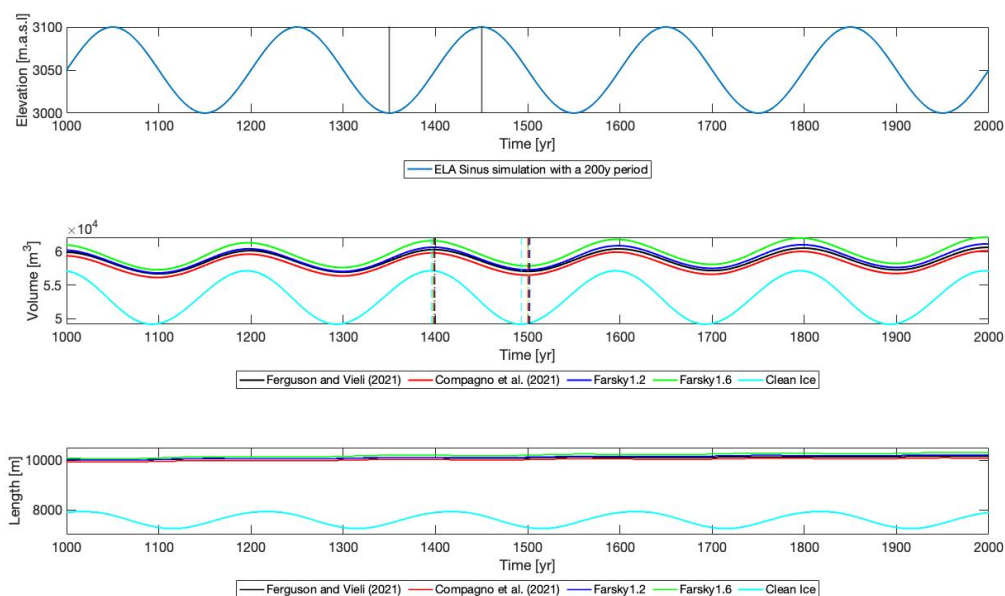


Figure 15. Length and volume fluctuations following a sinus experiment with a 200-year period.



---

An increase of the sinus period to 400 years mirrors a very similar pattern for the volume fluctuations. Maximum and minimum are lagging about 100 years behind the minimum and maximum of the ELA. It becomes a little more evident that glacier volume variations at the maximum for all given equations show more in-between variation than at the glacier minimum volume. In-between variation at a maximum is 1'877 m<sup>3</sup>, at the minimum only 656 m<sup>3</sup>.

Another very interesting pattern can be observed with the length fluctuations.

Reaction time to a decrease of the ELA happens much quicker than to an increase of the ELA with the response to an increasing ELA being more delayed and starting very slow. A minimum extent is reached 281-288 years after the ELA reached its highest elevation, reaching the maximum length to an ELA at a minimal elevation takes 217-237 years. Similar as deduced from the step change experiment, F2 reaches a steady length the quickest after glacier extent. The corresponding figure can be found in Appendix A6.

The time required for a glacier to go from a minimum extent to a maximum extent is almost exactly 200 years, which is half the period of the sine curve. This cannot be said for the length, where the same minimum-maximum change takes only 130 years. In contrast, the time needed for the glacier to go from its maximum to its minimum is 270 years.

For the 800-year sinusoidal period, the same patterns can be observed. Once more, a comparison to a clean ice glacier is involved as shown in figure 16. The most interesting information that can be taken from the plots is the delay difference between the clean ice and debris covered glaciers. The maximum volume and length for the clean ice glacier is reached 69 and 78 years after the coldest simulated temperature, respectively, whereas the debris covered glaciers need around 140 years to reach their maximum volume and around 250 years to reach a maximal length. Once reaching a maximum length, debris covered glaciers do not change their length for about 80 years before a reaction can be observed to the reduction in volume. The already mentioned in-between differences at maximum volume increases under an 800-year period even more to a difference of 2'680 m<sup>3</sup> between F2 and C. The in-between differences between these equations at the minimum volume is only 75 m<sup>3</sup>.

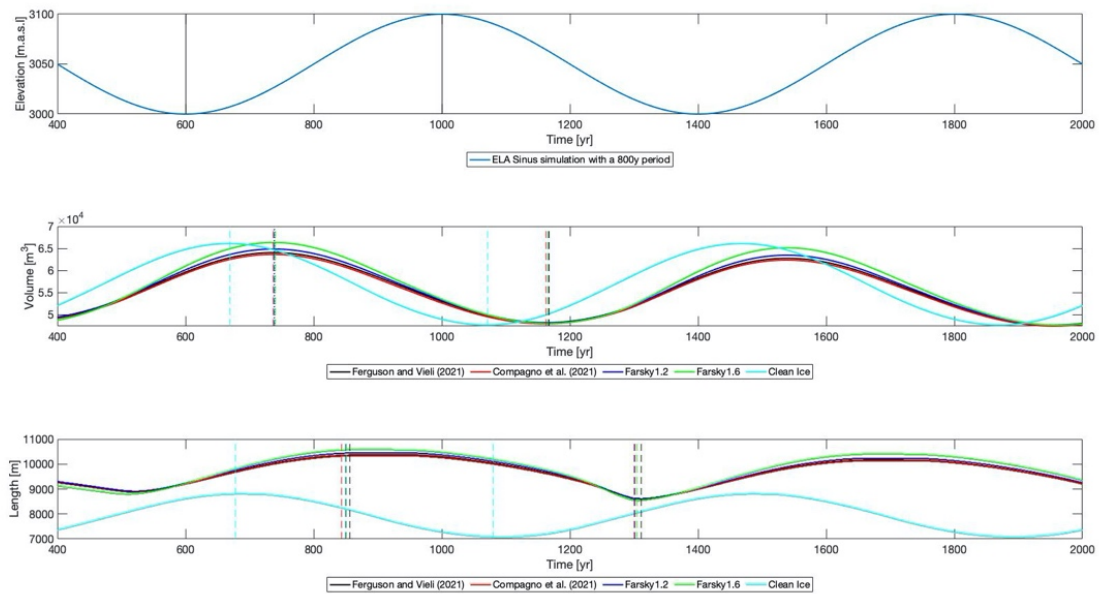


Figure 16. Length and volume fluctuations following a sinus experiment with an 800-year period.

A 1600-year period yields almost the same results. Given such a long time period, the length fluctuations start to resemble an almost sinus behaviour, notwithstanding the longer time the glacier stays in a maximum extent and a quicker increase in glacier length in response to a decreasing ELA.

#### 4.2.3 Gradual Increase of the ELA

Under a linear increase of the ELA, which is equal to a constant increase of temperature, the glaciers volume decreases in an inversed constant decline. The ELA increases based on the function  $y=0.8t+c$ , with  $t=1$  yr. The glaciers volume loss can be described by a function of  $y=-0.8t+c$ . At about 350 years, the volume has a sudden increased volume loss, which can be explained by the ELA reaching the steep head wall area (see figure 17).

Much more interesting is the length behaviour where a very sudden decrease in length can be observed after 330 years, which is the moment when the glacier collapses. The glacier retreats by 4000 meters in 70 years, which can be nicely seen in figure 18. Significant differences between the equations cannot be detected.

At the start of the linear decrease the glacier length significantly reduces as it hasn't adapted to the previous temperatures. The volume reacts much quicker to the decreased temperatures and starts increasing again.

The time span used for both experiments is 500 years. While the glacier loses almost 6000 m in length in this period, it gains only about 1000 m with a decreasing ELA.

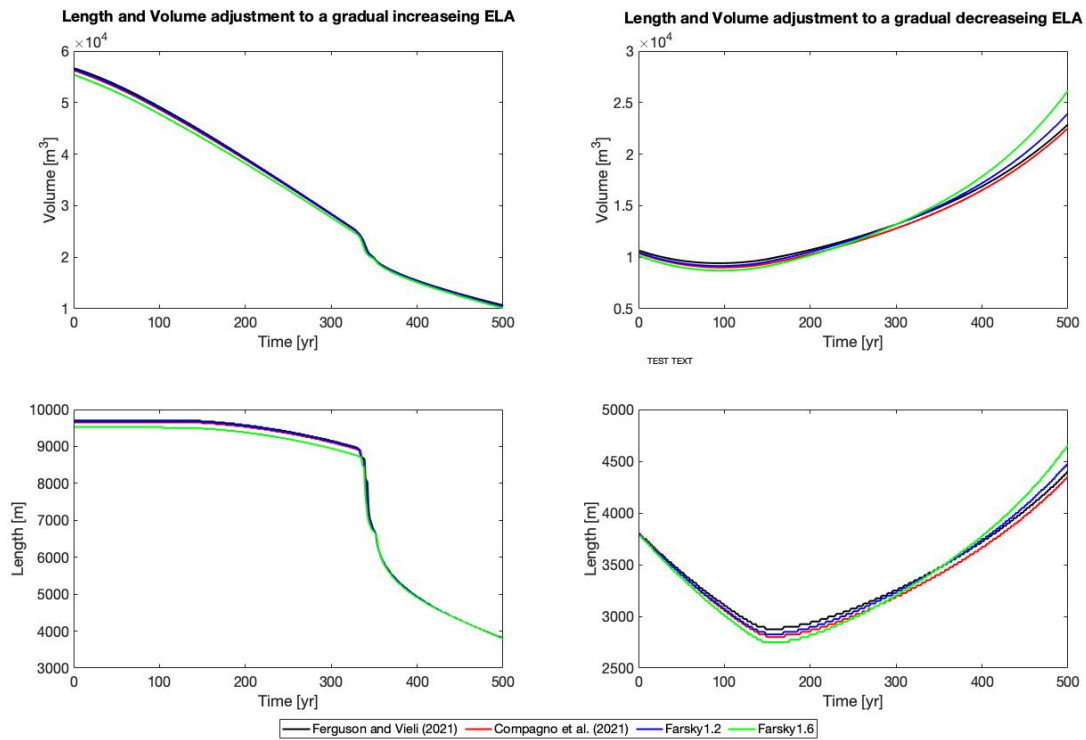


Figure 17. Length and volume adjustments to a constantly increasing ELA.

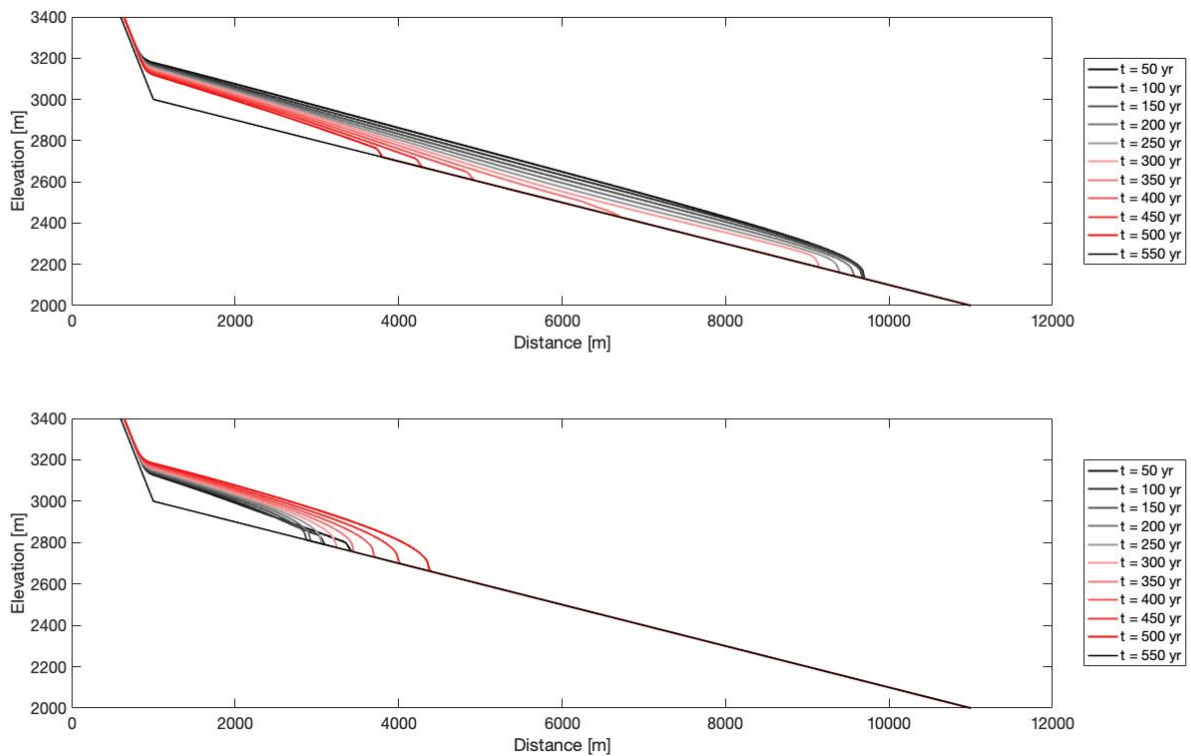


Figure 18. Glacier adjustments to a linearly changing ELA.

#### 4.2.4 ELA Forcing

The ELA forcing used in this example is provided by Lüthi et al. (2010). Based on glacier reconstructions, the ELA forcing should represent the temperature fluctuations since year 0 until 2030.

Based on the different magnitudes of enhanced melt, the four maximum volumes of the four glaciers differ slightly at the start of the experiment but the behaviour displayed throughout the experiment is equal for each glacier (see figure 19). It once more becomes evident that volume adjustments to the climate forcing are equally delayed for debris covered glaciers as well as for clean ice glaciers, with clean ice glaciers having stronger fluctuations. Glacier length on the other hand is much more reactive for a clean ice glacier, while debris covered glaciers do not show any assignable reaction to the ELA forcing. During the LIA, the period from 1600 to 1860, the volume increases in response to the cold phase. Since the end of the LIA, all glaciers show a similar reduction in mass. An interesting side note can be observed with the comparison to a clean ice glacier experiencing the same climate. While the length of a clean ice glacier shows a reaction to the warmer temperatures since the LIA, debris covered glaciers keep growing only to stagnate in the last couple of years.

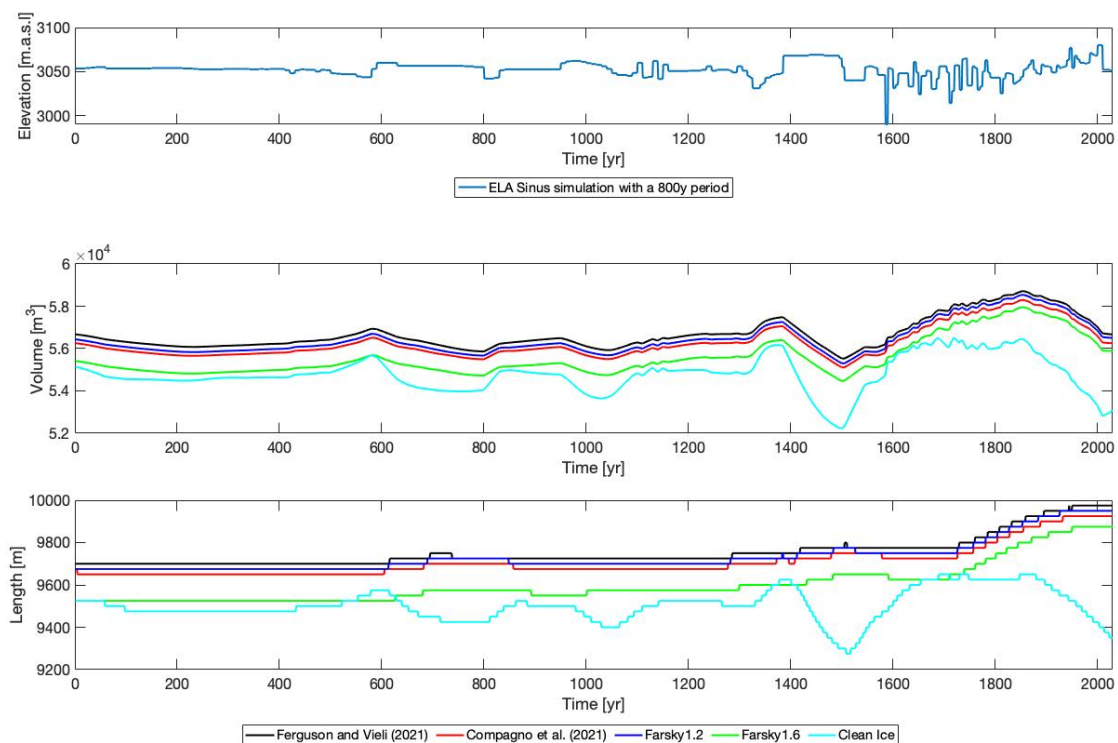


Figure 19. Length and volume adjustments to an ELA forcing representing Swiss Alpine historic climate variations.

#### 4.2.5 Debris Layer Transport

Of general interest when comparing the different equations is how the debris layer increases in thickness as we move downwards along the ablation area. The general behaviour of all four simulations, as shown in figure 20a, is very similar with an almost exponential increase in debris thickness, starting at the beginning at the ablation zone increasing to a maximum of about 1.4 m right before the terminus of the glacier ( $J_{\max\_D} = 1.45$  m;  $C_{\max\_D} = 1.44$  m;  $F1_{\max\_D} = 1.45$  m;  $F2_{\max\_D} = 1.36$  m). As the maximum possible debris thickness depends on total glacier length, a F2 simulation has the thinnest maximum debris thickness due to its higher melt enhancement. The most interesting information can be found when looking more closely at the beginning of the ablation area (see figure 20b), where first debris start to melt out. While the FV simulation has a constant increase until reaching the terminus, simulations C, F1 and F2 exhibit a quicker increase in debris thickness until reaching  $h_{\text{crit}}$  ( $h_{\text{crit}} = 0.03$  m), due to the inclusion of the enhancement factor. The zone of enhanced melt is the smallest for F2 with a length of 500 m, which equals 5.2 % of the total glacier length and 6.9 % of the complete debris layer. Values for the other simulations can be taken from table 6.

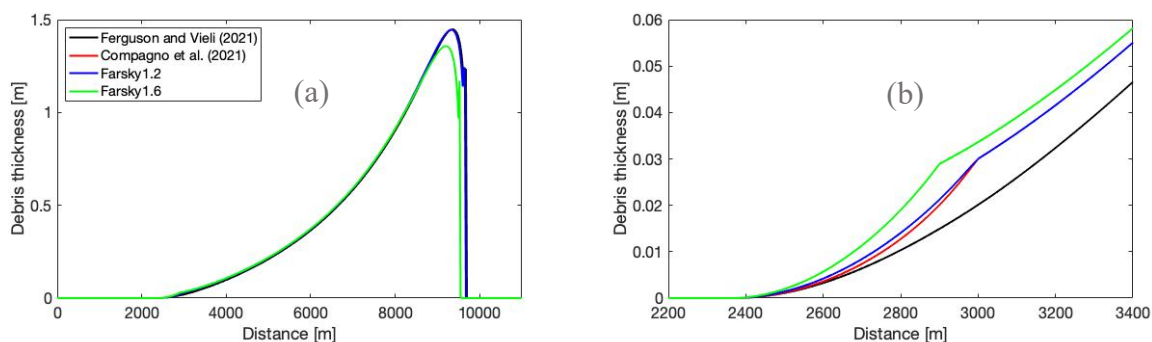


Figure 20. (a) Debris thickness evolution; (b) debris thickness increase at the beginning of the melt out zone.

Table 6. Properties of the debris zone with enhanced melt rate after a step change simulation

	<i>FV</i>	<i>C</i>	<i>F1</i>	<i>F2</i>
Glacier length after step change 3050 → 3100 m [m]	8325	8325	8325	8275
Length of complete debris area [m]	6475	6475	6475	6450
Length of zone with enhanced melt after step change 3050 → 3100 m [m]	625	500	500	425
relative length to total glacier [%]	7.5	6	6	5.1
relative length to total debris area [%]	9.6	7.7	7.7	6.6
Glacier length after step change 3100 → 3050 m [m]	9700	9675	9675	9575
Length of complete debris area [m]	7325	7325	7325	7225

<i>Length of zone with enhanced melt after step change 3100 → 3050 m[m]</i>	725	550	575	500
<i>relative length to total glacier [%]</i>	7.5	5.7	5.9	5.2
<i>relative length to total debris area [%]</i>	9.9	7.5	7.9	6.9

Given that we know the exact length of the zone with enhanced melt rate (0-0.03 m), it is of interest to test how this zone reacts to changes of the ELA. In figure 21 we can see (1) how quickly the area of enhanced melt adjusts to a step change (ELA from 3050 → 3100 m and back from 3100 → 3050 m) as well as (2) the actual length of this zone. To have a point of comparison, the FV simulated debris layer of 0-0.03 m is also included. Figure 21 confirms the findings of figure 20b, indicating that the debris thickness zone ranging 0-0.03 m is the largest for FV, equally long for C and F1, and the smallest for F2, due to its higher enhancement. All models display a similar adjustment time of roughly 50 years to reach again to a constant length of this zone. Whilst during a step increase of the ELA the zone temporarily increases to about 1000 m in length, it decreases to a temporary length of only 375 m for a F2 simulated glacier under a step decrease of the ELA (see figure 22). The zone of enhanced melt keeps growing for about 120 years, which agrees with earlier findings that a glacier adjusts quicker to an increase in temperature than to decreasing temperatures.

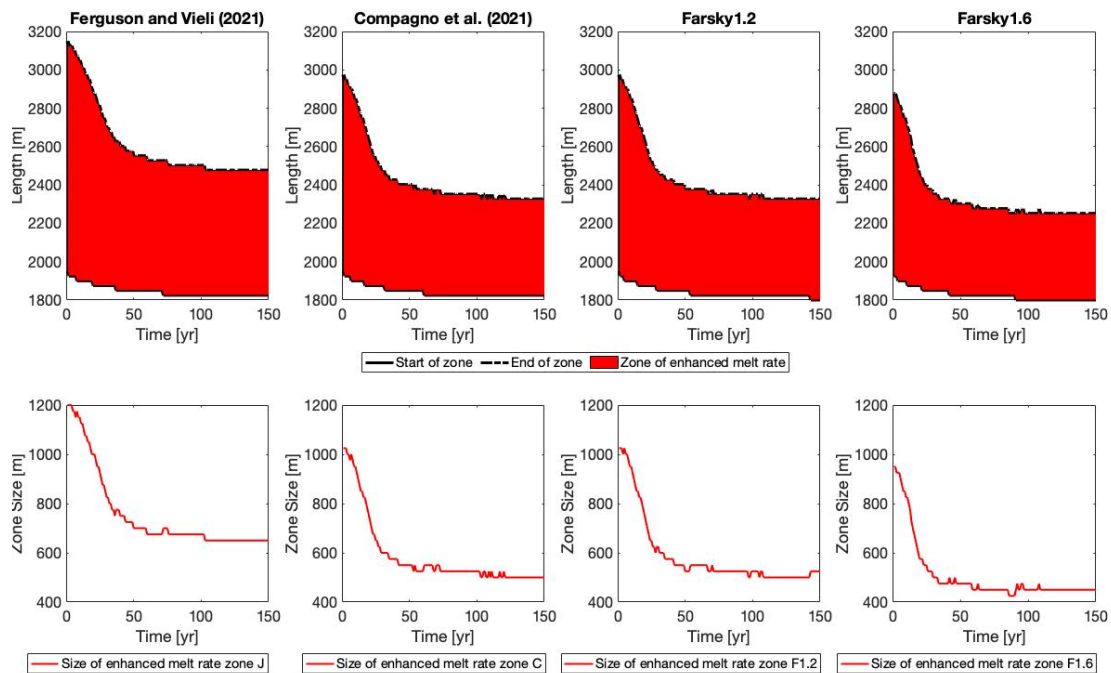


Figure 21. Zone of enhanced melt rate adjustment to an ELA step change from 3050 m to 3100 m.

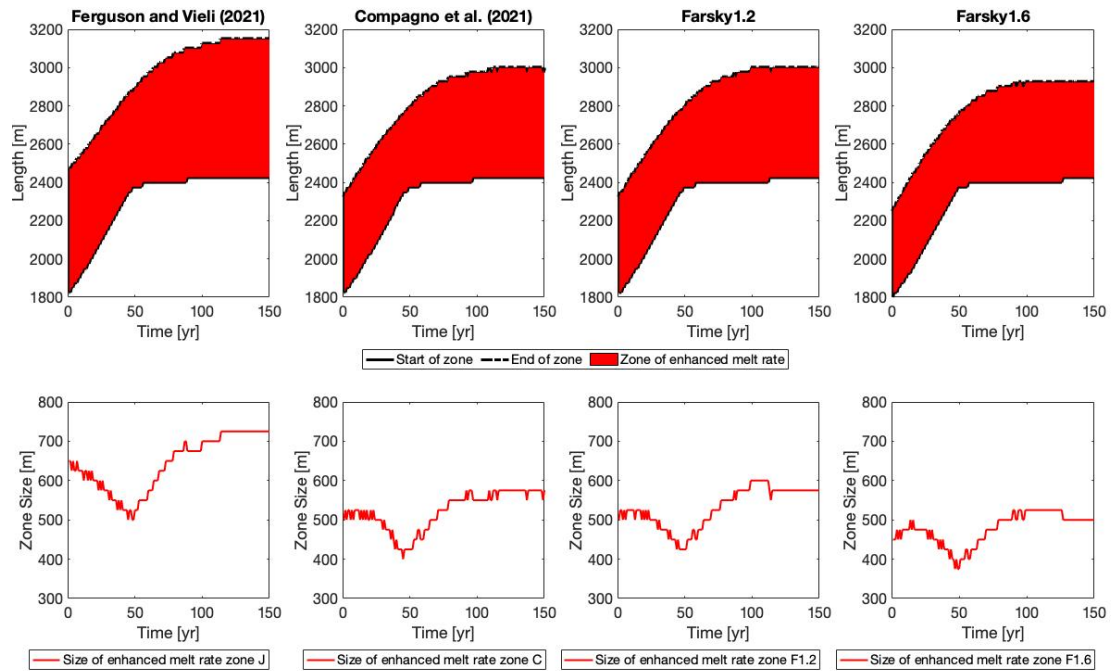


Figure 22. Zone of enhanced melt rate adjustment to an ELA step change from 3100 m to 3050 m.

#### 4.2.5.1 Step change simulation under an increased slope of 20°

The purpose of this experiment is to see how the enhanced melt rate zone changes for a glacier with a 20° bed geometry instead of a 10° bed geometry. The ELA is kept at the same elevation of 3050 m. Given the steeper slope, the glacier's maximum extent is with 4900 m 38 % shorter than a glacier under a bed geometry of 10°. Performing a step change experiment, we can again analyse how the zone of enhanced melt changes as summarised in table 7. Similar to a step change experiment with a 10° bed geometry, the zone keeps proportionally the same length relative to the entire glacier extent. The relative length of the zone of enhanced melt, however, does increase in comparison to a 10° slope by about 4 %, indicating that the relative size of this zone increases for glaciers with a steeper slope. Despite the increased proportion of the enhanced melt zone of the entire glacier, this has little effect on the length and volume of the glacier with differences mostly within the grid differences of 25m. However, it might be significant for shorter glaciers. With the glaciers being much shorter, adjustment times are also reduced and the zone of enhanced melt reaches its final length faster than a larger glacier would (see Appendix A8).



Table 7. Properties of the debris zone with enhanced melt rate after a step change simulation with a slope geometry of 20°

	<i>FV</i>	<i>C</i>	<i>F1</i>	<i>F2</i>
<i>Glacier length after step change 3050 → 3100 m [m]</i>	4575	4575	4550	4500
<i>Length of complete debris area [m]</i>	3500	3500	3475	3425
<i>Length of zone with enhanced melt after step change 3050 → 3100 m [m]</i>	525	400	400	350
<i>relative length to total glacier [%]</i>	11.5	8.7	8.8	7.8
<i>relative length to total debris area [%]</i>	15	11.4	11.5	10.2
<i>Glacier length after step change 3100 → 3050 m [m]</i>	4900	4875	4785	4800
<i>Length of complete debris area [m]</i>	3575	3550	3550	3475
<i>Length of zone with enhanced melt after step change 3100 → 3050 m [m]</i>	550	425	425	350
<i>relative length to total glacier [%]</i>	11.2	8.7	8.7	7.1
<i>relative length to total debris area [%]</i>	15.4	12	12	10.1

#### 4.2.5.2 Step change simulation under a warmer climate (ELA: 3150 → 3200 → 3150 m)

This experiment's purpose is another approach to see if the area of enhanced melt rate stays equally large in comparison to the total glacier length, independent of the glacier length. To test this, a simple step change experiment was conducted with a glacier building up under a constant ELA of 3150 m.a.s.l. For the step change, the ELA is changed to an elevation of 3200 m and in a last phase back to 3150 m.

After reaching a steady state under a constant ELA of 3150 m, the zone of enhanced melt takes up between 6.5 to 9.6 % of the entire glacier, which is an average increase of 1.8% in comparison to a glacier under a constant ELA of 3050m. This variance can most likely be neglected, as variance due to the spatial discretization can be seen as the origin. Other than that, the glacier behaves similar as a glacier under a steady ELA of 3050 m.

Table 8. Properties of the debris zone with enhanced melt rate after a step change simulation with ELA changes of 3150 m  $\rightarrow$  3200 m  $\rightarrow$  3150 m

	<i>FV</i>	<i>C</i>	<i>F1</i>	<i>F2</i>
<i>Glacier length after step change 3150 <math>\rightarrow</math> 3200 m [m]</i>	5775	5775	5775	5700
<i>Length of complete debris area [m]</i>	4975	4975	4975	4900
<i>Length of zone with enhanced melt after step change 3050 <math>\rightarrow</math> 3100 m [m]</i>	425	300	300	225
<i>relative length to total glacier [%]</i>	7.4	5.2	5.2	4.0
<i>relative length to total debris area [%]</i>	8.5	6.0	6.0	4.6
<i>Glacier length after step change 3200 <math>\rightarrow</math> 3150 m [m]</i>	6275	6275	6275	6175
<i>Length of complete debris area [m]</i>	5100	5100	5100	5000
<i>Length of zone with enhanced melt after step change 3100 <math>\rightarrow</math> 3050 m [m]</i>	600	475	475	400
<i>relative length to total glacier [%]</i>	9.6	7.6	7.6	6.5
<i>relative length to total debris area [%]</i>	11.8	9.3	9.3	8.0

#### 4.2.6 Step change with different $D_0$ of $D_0=0.1$ m

The purpose of this experiment is to see if the parameter  $D_0$  can be chosen at random or if different values have a substantial effect on variability between the different approaches to calculate SMB. To investigate this, a step change experiment was carried out with a characteristic debris thickness of 0.1 m instead of 0.05 m as was utilized in all previous experiments. While a value of 0.1 m correlates best with the data collected during the field work on Zmuttgletscher in summer of 2021, a value of 0.05 m for the free parameter  $D_0$  has been used in previous modelling approaches, among others by Ferguson and Vieli (2021). With a larger  $D_0$ , all simulated glaciers become significantly shorter and smaller in volume (see figure 23). The glacier loses 2000 m in length and about 12'000 m<sup>3</sup> in volume. Aside from that, simulated glaciers with a characteristic debris thickness  $D_0 = 0.1$  m do not differ significantly from simulated glaciers with a characteristic debris thickness  $D_0 = 0.05$  m. Differences are mostly due to the 25 m grid size resolution. With an overall smaller size, the glacier reaches its steady states after a step change to 3100 m 200 years earlier as would a larger glacier with  $D_0 = 0.05$  m.

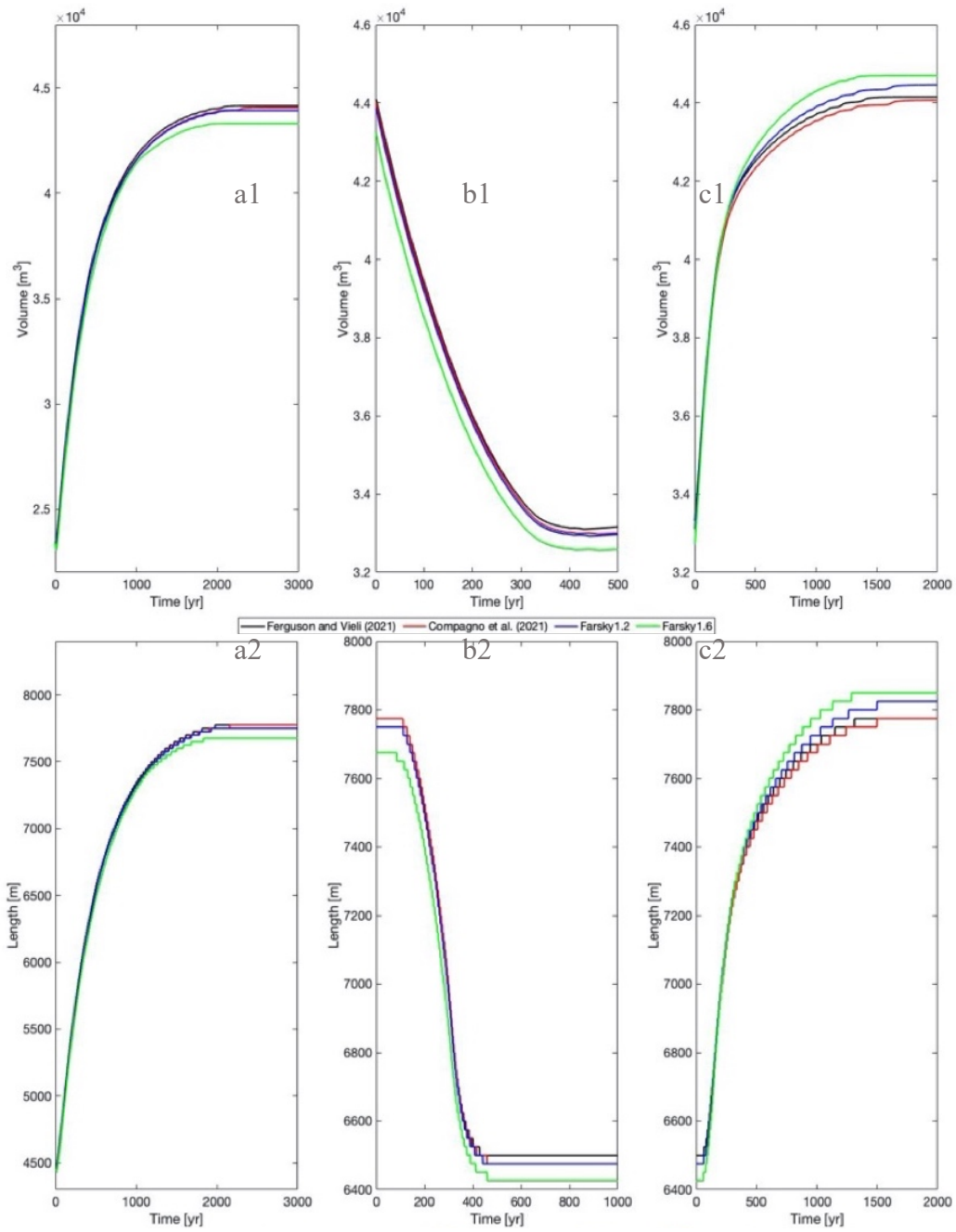


Figure 23. Length and volume change after a step change experiment (ELA: 3150 → 3200 → 3150 m).

---

#### 4.2.7 Summary of modelling results

Based on the modelling experiments, a short summary comprised of the most important results is given.

- 1) Discrepancies between the four proposed SMB computation methods are almost non-existent. Independent of the simulation type, all glaciers react very similar and in-between volume and length variations are mostly due to the spatial discretization of the grid.
- 2) A glacier reaches its steady state much quicker while retreating than after expanding
- 3) After an increase in temperature, the volume shows an instant reaction, whereas a reduction in length is delayed.
- 4) After a decrease in temperature, both volume and length increase directly.
- 5) A debris covered glacier prefers to grow instead of reducing its length and thus, reacts quicker to a temperature drop than to an increase in temperature
- 6) Zone of enhanced melt rate is shorter, the higher the enhancement effect
- 7) Zone of enhanced melt rate stays proportional to the total glacier length under the same geometry; on average, it takes up about 7 % of the entire glacier surface
- 8) Under a constant temperature, glaciers with enhanced melt tend to be smaller. After strong temperature fluctuations glaciers with enhanced melt seem to get larger than glaciers without enhancement

---

## 5 Discussion

### 5.1 Implications of field measurements

The ablation measurements taken on Zmuttgletscher indicate an Østrem-like behaviour with ablation for partially covered surfaces being enhanced by as much as 20 %, whilst thick debris layers were found to reduce ablation by as much as 61 %. These values vary throughout the literature but are well within range of other studies (Østrem, 1959; Loomis, 1970; Small and Clark, 1974; Fyffe et al., 2020). Similar as Fyffe et al. (2020) and Nicholson and Benn (2006) concluded in their respective studies, enhanced melt can only be attributed to partially covered surfaces, which makes the possible surface area with enhanced melt quite small. Additionally, enhancement for partially covered surfaces or even thin fully covered surfaces in comparison to the clean ice case may only be detectable if the clean ice surface is sufficiently free of debris or dirt ice (Fyffe et al., 2020). Surfaces classified as clean ice on Zmuttgletscher still displayed a small amount of dirt ice, resulting in a possible higher ablation due to an increase in incorporated net shortwave radiation.

An inverse relationship exists between albedo and ablation for partially covered surfaces, with lower percentage coverage surfaces having a greater albedo while an increase in percentage coverage results in a decrease of albedo (see figure 11a) (Azzoni et al., 2016). The four partially covered surfaces analysed in this study have a similar melt enhancement, which is explained by Fyffe et al. (2020) to be caused by an interaction between an increase in intake of net shortwave radiation and a simultaneous increase in clast size, responsible for a reduction in ablation.

The justification behind this is based on data collected by Fyffe et al. (2020), as seen in figure 24's left plot. It clearly shows that the enhancement is very similar for all levels of percentage coverage, while melt rates for fully covered surfaces can take on a wide range of possible values. Based on this plot, a similar plot was created with the data collected on Zmuttgletscher. While only a few measurements were taken on partially covered surfaces, the general pattern is very similar and thus, supports the findings of Fyffe et al. (2020).

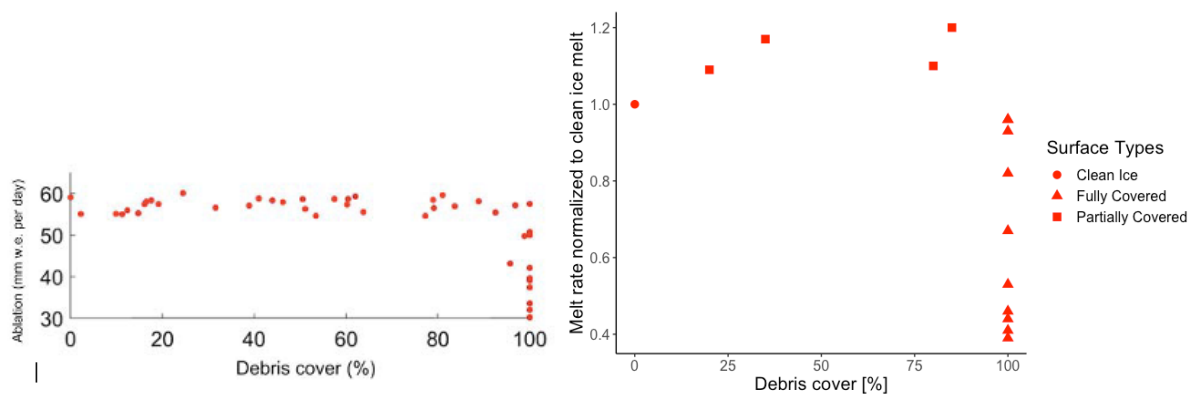


Figure 24. Ablation against debris cover. Comparison of (a) results from Fyffe et al., 2020. and (b) results from this study.

A possible question this thesis ought to answer is whether changes in layer thickness can be detectable within a short time frame of a month. Most changes were found to range within a 2 cm error range, possibly caused by inaccuracies while taking measurements. Nonetheless, it cannot be ruled out that the observed variances in debris thickness are attributable to changes in clast arrangement, which can be seen in every location from aerial picture comparisons (see Appendix A1). While measurement error can be used as a good explanation for most of the changes, changes at 5D and 13D must have a different cause. The location around 13D experienced a decrease in debris thickness of 7.8 cm. With a slope angle of  $15^\circ$ , 13D has the steepest and only positive slope angle, which could result in heavier surface rearrangements following significant rainfall events or single clasts losing integrity due to surface melt, resulting in the found debris thickness loss.

While these factors may also play a role in the development of 5D, it is more likely that the area surrounding 5D was subjected to melt out. Visibly, the area changed as one can see in figure 10 with a general increase in clast size free on the surface. With an aspect angle of  $108^\circ$ , 5D is the only surface facing east, experiencing a more direct angle of incoming solar radiation. With a higher incoming net radiation, melt out might be accelerated and actually cause a surface to change its effect on SMB within a short time frame due to melt out. As most areas of Zmuttgletscher face due north, only fringe areas near the moraines should be affected by this circumstance. Unfortunately, 5D is the only surface analysed that had a layer thickness of below a centimetre and that experienced for a short time a higher melt rate than the clean ice surface. As a result, it's impossible to rule out the possibility that thin debris layers can increase in a short period of time.

---

## 5.2 Implications of modelling experiments

The field data provided an additional equation to use for the simulation of debris covered glaciers with enhanced melt rates for thin debris layers. While the data obtained on Zmuttgletscher can be used to produce an Østrem curve, it cannot be utilized to determine a useful value for the critical debris thickness. Due to the model's inability to depict partially covered surfaces, a value of  $h_{\text{crit}} = 0.03$  m was selected based on data from previous studies (Loomis, 1970; Small and Clark, 1974; Compagno et al., 2021). For the range of  $<0$  to 0.03 m two equations were used to integrate enhanced melt into the DEBISO model. While two simulations employed a constant enhancement factor (1.2x and 1.6x) for this range, an equation proposed by Compagno et al. (2021) was implemented that takes on varied enhancement values for this range, culminating at 0.03 m.

After comparing simulations where SMB is calculated with and without enhancement, the results strongly suggest that the inclusion of increased melt is a negligible factor for future debris-covered glacier modelling studies. All four approaches react very similarly to applied experiments with in-between differences in volume and length being very small and mostly due to the spatial discretization of the grid. Differences between inclusions of enhancement and no enhancement are highest between simulations FV and F1.6, which can simply be explained by F1.6 having the highest enhancement factor of 1.6 times the clean ice melt. While the differences are minimal, it is worth noting that F1.6 has the fastest response to ELA changes and the fastest time to establish a steady state. Both findings can be attributed to the higher enhancement factor. During a glacier retreat, the zone of enhanced melt grows slightly, resulting in a higher SMB and thus, an earlier response. On the other hand, when a glacier expands, the zone of enhanced melt shrinks, resulting in a larger area being better insulated and a faster growth, causing the glacier to achieve its steady state sooner.

A possible explanation for why all four approaches yield relatively similar results despite the inclusion of enhanced melt can be given when taking a closer look at the zone of enhanced melt (debris layer ranging in thickness from  $<0$  to 0.03 m). The higher the enhancement factor, the shorter this zone becomes with the F1.6 simulation having a 200 m shorter zone of enhanced melt as a glacier experiencing direct insulation (figure 20b; 21; 22).



With a much smaller debris zone ranging from 0 to 0.03 m, a glacier with enhanced melt experiences stronger insulation sooner along the ablation zone, which offsets the effect of the zone's increased melt rate, resulting in almost equally long and voluminous glaciers.

It is also worth noting that this zone is only about 400-600 meters long, accounting for approximately 6-10 percent of the glacier's total debris area. Taking up only such a small fraction of the entire debris area, minor changes as caused by the inclusion of enhanced melt, turn out to be negligible. Another reason why the enhanced melt zone does not contribute to major changes is that the zone shrinks to its final length within 50 years following a step change, giving the enhancement effect no opportunity to exhibit any meaningful effects on SMB as shown in figure 25. Figure 25 demonstrates how quickly the enhanced melt zone responds to the new set ELA after a step change. Within 50 years, the zone has almost reached its steady state length after an increase of the ELA. After a decrease of the ELA, reaching a steady state for the zone of enhanced melt takes about 100 years.

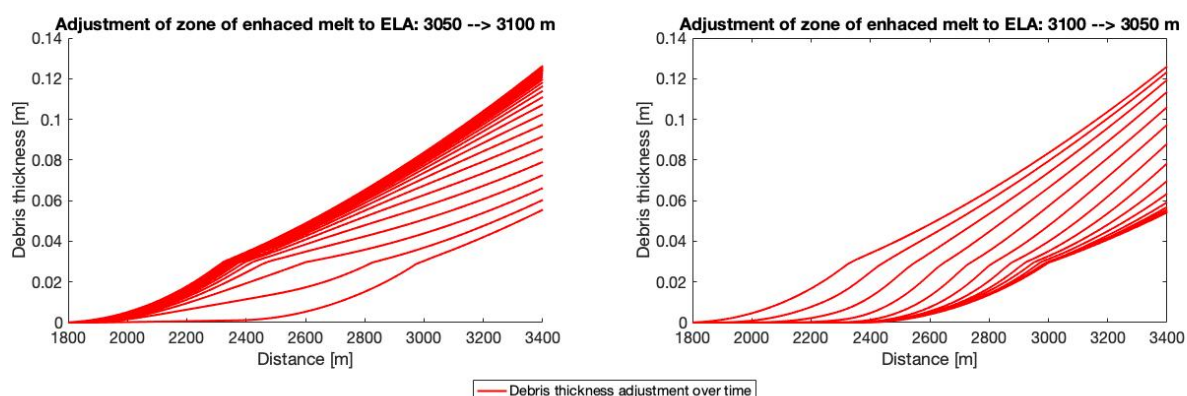


Figure 25. Adjustment of debris layer to step change experiments. Debris layers are plotted in 10-year steps.

To test whether the zone of enhanced melt stays proportionally the same in size independent of the glacier length, the zone was analysed for glaciers in steady states under different climate conditions. The changes discovered under different climate conditions for glaciers with the same bed geometry are very small and they have no substantial effect on general adjustment time or reaction time for the four approaches calculating SMB. Steady state glacier volume and length remain similar for all approaches. The existing differences can most likely be explained by the spatial discretization used in the model.

While the zone of enhanced melt stays proportional for glaciers independent of their length, it is important to point out that differences were found for glaciers under different bed geometries. The results suggest that the enhanced melt zone increases by about 4 - 5 % to roughly 10% -

---

15% for glaciers with a steeper bed geometry of 20° instead of 10°. Despite the fact that the zone takes a larger share for steeper glaciers, the variations between the four approaches are still minor and do not necessitate the inclusion of accelerated melt in future modelling approaches.

### 5.3 Additional Implications

While the primary purpose of this investigation was to determine whether or not the addition of enhanced melt significantly alters SMB, it also yielded a variety of other findings, which are going to be covered in this section.

Given that this study utilized the same numerical model as Ferguson and Vieli (2021) have, similar results are expected.

All four approaches of simulating SMB presented a similar response to the step change experiment with the glaciers reaching their steady state much faster after a temperature increase as after a temperature decrease. While the glacier needs about 400 years to adjust volume and length after a step change from 3050 m to 3100 m, it takes 1300 to 1500 years to adjust volume and length following a step change from 3100 m to 3050 m (see figure 14 & 23). The asymmetric adjustment time can be explained by the quick adjustment in volume after an increase in temperature. While the tongue stays stationary for a while due to the strong insulation of the thick debris layer, the glacier's volume reduces similarly as a clean ice glacier. This is because warming has its strongest impact on the upper accumulation area and the beginning of the ablation area where debris are thin. When reaching a certain critical volume, the glacier length collapses and reaches an adjusted length to the new ELA within a very short period. During a glacier advance, the glacier must produce more mass in order to grow, which takes significantly longer.

It is clear from the step change experiment, and even more so from the sinus experiment, that volume and length respond to ELA forcing in different ways (see figure 14 & 15). While the volume of the glacier responds almost immediately to a step change from 3050 to 3100 m, the length of the glacier takes 150 to 180 years to respond to such a step change. During a step change where the ELA is decreased to 3050 m again on the other hand, both length and volume show an almost immediate response (see figure 26). The delayed response of the glacier's

length can be explained by the strong insulation effect of the debris layer. Towards the terminus, the debris layer is almost 1.5 m thick providing enough protection that moderate temperature changes have no effect on glacier length. Given enough time after a step change, the glacier loses that much volume that the glacier almost collapses and drastically decreases in length as shown in figure 26.

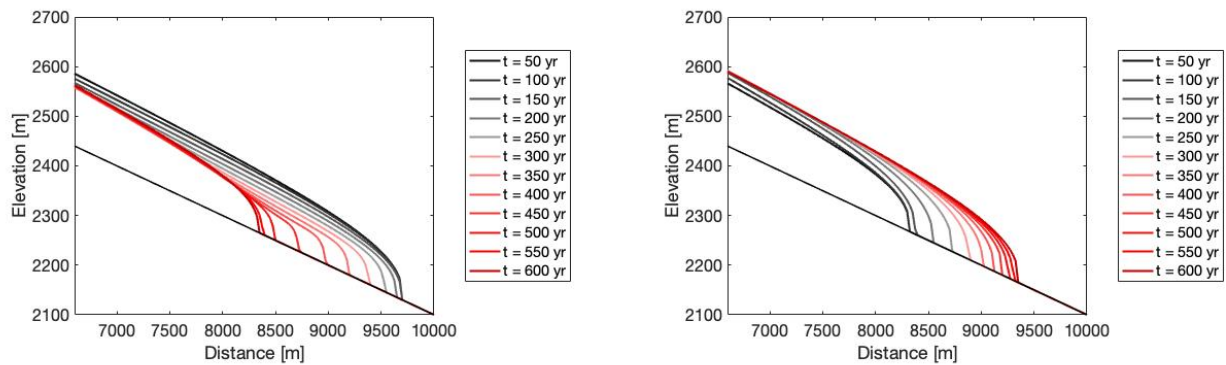


Figure 26. Glacier adjustment to a step change of (a) the ELA 3050  $\rightarrow$  3100 m in a 50-year step and (b) ELA 3100  $\rightarrow$  3050 m.

Taking a closer look at the sinus simulations (figure 15), it also becomes noticeable that the glacier's maximum length and volume grow slightly with each period, which would be indicative for a hysteresis. According to Ferguson and Vieli (2021), this does not equate a proper hysteresis however, as the glaciers would reach a unique steady state given several centuries time to adjust. In reality, this indicates that the length of a debris-covered glacier is governed by the history of successive cold episodes rather than the glacier having a unique steady state for a given climate (Ferguson and Vieli (2021)).

Results presented using the ELA forcing by Lüthi et al. (2010), where debris covered glaciers are compared with a clean ice glacier, complement empirically observed data from Quincey et al., (2009), Scherler et al., (2011) and Ragettli et al., (2016). Many debris covered glaciers tend to have stagnant tongues with no significant adjustments to global warming whereas clean ice glaciers show unambiguous adjustments. This can be observed when looking at figure 19, where length and volume responses to the ELA forcing are plotted. While the length and volume of a clean ice glacier adjust quickly to a warming climate, debris-covered glaciers have only responded to the LIA with a volume loss thus far. This agrees with observations of high mass loss for all kind of glaciers independent of debris cover or clean ice (Pellicciotti et al., 2015). It also agrees with the modelling results from Compagno et al. (2021). Based on the

---

assumption that debris-covered glaciers remember prior colder temperatures better than warmer temperatures, it appears that the impacts of the LIA are still affecting the length of debris covered glaciers. These findings are consistent with those of Banerjee and Shankar (2013) and Compango et al. 2021, who found that glaciers classified as stationary are still losing volume and that a glacial retreat is likely as soon as a maximum debris cover is attained resulting in a disintegration of the debris covered tongue.

#### 5.4 Limitations

The field data was sufficient to represent a true Østrem curve with partially covered surfaces representing the rising limb. Nevertheless, more data points for partially covered surfaces as well as for thin debris layers (0.5-1.5 cm) would have been beneficial. The data points do not allow for the determination of a critical debris thickness but suggest that only partially covered surfaces display enhanced melt. With measurement point 5D however, a possible fully covered location was measured that, for a short while, had a higher ablation rate than clean ice. Given this finding as well as findings of other studies (Loomis, 1970; Small and Clark, 1974; Konovalov, 2000; Popovin and Rozova, 2002), it cannot be ruled out that fully covered surfaces can also have a higher ablation than clean ice. Most likely it is not possible to determine a unique value for the critical debris thickness however, as local climate, environmental factors as well as lithology of the debris can have an impact on the effects of debris cover. Difficulties in specifying a unique value for the critical debris thickness in the field starts already with finding clean ice surfaces to normalize melt rate of covered surfaces. As Fyffe et al. (2020) mentioned, most clean ice surfaces encountered in the field are not 100% clean and thus, do alter possible results. A feasible technique to present clean ice surfaces as well as thin debris covered surfaces would be to artificially change the glaciers surface to one's liking to better represent the surface types of interest.

Given the findings of this study as well as the study from Fyffe et al. 2020, it becomes more evident that future research should be directed to partially covered surfaces as these display enhanced melt rates in comparison to clean ice. Most fully covered surfaces experience insulation. Since this correlation is empirically supported, the importance of such areas for surface mass balance calculations seem most important. While in-situ measurements can be difficult to perform, remote sensing could be applied to analyse the patchiness of glacier surfaces classifying surfaces based on rock or ice. Under a time-series, this approach could analyse the dynamic of surface change, how quickly melt out can occur as well as calculate the

---

overall share of partially covered surfaces. Given this knowledge, numerical models could be adjusted by integrating the patchiness of debris covered glaciers.

The DEBISO model employed in this thesis is a well-tested numerical model that can moderately replicate real-world glaciers while capturing the correct ice physics (Ferguson and Vieli, 2021). Nevertheless, it uses many simplifications that limit the real-world application. One of such simplifications is the use of a continuous and homogenous distribution of debris. As the field work on Zmuttgletscher showed, it is possible to find areas of clean ice and areas of fully covered surfaces with a debris thickness of 10-15 cm within short distance on roughly the same elevation. This is due to a non-homogenous debris deposition of the surrounding headwalls. Similarly, clast sizes can vary from a few millimetres to more than 1 m. Additionally, the englacial transport of debris is not implemented in this model, resulting in all debris melting out at the ELA, which is an acceptable approach for debris covered glaciers where debris are deposited near the ELA but not for debris covered glaciers where debris deposition happens far above the ELA (Ferguson and Vieli, 2021).

Under current setting of the model, with a simplified bed geometry, it seems that the inclusion of enhanced melt can be neglected. Given a real-world scenario, a glacier bed is very uneven, consisting of small valleys, ridges, possible sub-glacier lakes and other surface types that could result in greater differences between simulations including enhanced melt and simulations without enhanced melt. Effects of cryokarst, which can have significant impacts on surface melt, are also neglected.

Finally, the zone of enhanced melt was selected to represent any debris layer ranging from  $<0$  to 0.03 m based on findings of various studies (Loomis, 1970; Small and Clark, 1974; Compagno et al., 2021). However, the findings of this study as well as findings from Nicholson and Benn (2006) and Fyffe et al., (2020) discovered that enhanced melt is only found for partially covered surfaces. Such surfaces are, as of yet, not integrated in any numerical models. In order to more accurately reflect empirical findings, a new approach to integrate patchiness of debris layers contributing to accelerated melt would be beneficial for future modelling studies.

---

## 6 Conclusion

The present study presents a first approach in implementing increased melt in numerical melt models. Enhanced melt was calculated based on two equations, one postulated by Compagno et al., (2021) and one using a constant enhancement factor calculated from fieldwork on Zmuttgletscher for an area where debris layers are thinner than a critical debris thickness. Variable ELA forcing experiments showed that the differences for modelled glaciers with and without enhancement do not differ significantly and that enhanced melt only affect length and volume on a very small scale with response time and adjustment times to be very similar. While the differences are insignificant, it is worth noting that the higher the enhancement factor, the shorter and less voluminous the glaciers become. Variable ELA forcings cause these glaciers to react faster and attain their steady states sooner.

Ablation measurements from Zmuttgletscher indicate that increased melt is with 1.2 times the clean ice melt only found for partially covered surfaces. Due to the fact that only partially covered surfaces have enhanced melt rates, a new method for determining the surface area impacted by enhanced melt must be developed.

The method to integrate enhanced melt described above is a first step toward more precise simulations of surface mass balance for debris-covered glaciers, and the findings are likely applicable to any debris-covered glaciers of varying magnitudes.

---

## 7 Acknowledgments

This work would not have been possible without the assistance and contributions of a large number of individual people. First and foremost, I want to express my gratitude to Andreas Vieli for providing me with the chance to write this thesis, for assisting me in the development of the thesis from beginning to end, and for his support and feedback during countless meetings in the last year. Also, a big thank you to Boris Ouvry for all of his support, especially during the fieldwork, but also for always being there to answer any questions I had. In this regard, I also want to thank Florian Hardmeier for joining me to the fieldwork on Zmuttgletscher, for helping me conducting my measurements, giving me ideas as well for simply being around to chat and discuss about the topic.

Further, I'd like to express my thanks to Madelaine Schuler for her invaluable assistance working with MATLAB, which has helped me better understand the software as well as how to program in general.

At the University of Zurich, countless hours were spent in the “Masterarbeitsraum”. I want to thank all the people who spent time in this room with me, struggling, discussing and fooling around. In particular, I want to thank Jonas Michel for being a great roommate with whom I could discuss everything, be it scientific or intellectual.

Additionally, I want to thank Alexander Hess and Jonathan Davidson for proofreading my thesis as well as for helping me taking off my mind of the topic every now and then.

Finally, I want to express my gratitude to my parents for enabling me to pursue my academic studies at the University of Zurich for all of these years, as well as for encouraging and supporting me throughout the process of this thesis.



---

## 8 Bibliography

Adhikary S, Nakawo M, Seko K, Shakya B. (2000). Dust influence on melting process of glacier ice: experimental results from Lirung Glacier, Nepal Himalayas. *Debris Covered Glaciers: IAHS 264*: 43–52. <https://doi.org/10.1111/insp.12083>

Anderson, L. S., & Anderson, R. S. (2016). Modeling debris-covered glaciers: Response to steady debris deposition. *Cryosphere*, 10(3), 1105–1124. <https://doi.org/10.5194/tc-10-1105-2016>

Anderson, L., Anderson, R., Buri, P., & Armstrong, W. (2019). Debris cover and the thinning of Kennicott Glacier, Alaska, Part A: in situ mass balance measurements. *The Cryosphere Discussions*, 1–28. <https://doi.org/10.5194/tc-2019-174>

Anderson L. S. (2014). *Glacier response to climate change: Modeling the effects of weather and debris-cover* | Publications | Research | INSTAAR | CU-Boulder. <https://instaar.colorado.edu/research/publications/theses-dissertations/glacier-response-to-climate-change-modeling-the-effects-of-weather-and-debr/>

Anderson, L. S. and Anderson, R. S. (2016). Modeling debris-covered glaciers: response to steady debris deposition, *The Cryosphere*, 10, 1105–1124, <https://doi.org/10.5194/tc-10-1105-2016>

Azzoni, S.R., Senese, A., Zerboni, A., Maugeri, M., Smiraglia, C., & Adele Diolaiuti, G. (2016). Estimating ice albedo from fine debris cover quantified by a semi-automatic method: The case study of Forni Glacier, Italian Alps. *Cryosphere*, 10(2), 665–679. <https://doi.org/10.5194/tc-10-665-2016>

Banerjee, A., & Shankar, R. (2013). On the response of Himalayan glaciers to climate change. *Journal of Glaciology*, 59(215). <https://doi.org/10.3189/2013JoG12J130>

Benn, D. I., & Evans, D. J. A. (2010). *Glaciers & Glaciation: Vol. No. 2.*

Britannica, T. Editors of Encyclopaedia (2020, July 9). Albedo. *Encyclopedia Britannica*. <https://www.britannica.com/science/albedo>

Brook, M. S., Hagg, W., & Winkler, S. (2013). Debris cover and surface melt at a temperate maritime alpine glacier: Franz Josef Glacier, New Zealand. *Http://Dx.Doi.Org/10.1080/00288306.2012.736391*, 56(1), 27–38. <https://doi.org/10.1080/00288306.2012.736391>

Casty, C., Wanner, H., Luterbacher, J., Esper, J., & Böhm, R. (2005). Temperature and precipitation variability in the European Alps since 1500. *International Journal of Climatology*, 25(14), 1855–1880. <https://doi.org/10.1002/joc.1216>

Compagno, L., Huss, M., Miles, E. S., Mccarthy, M. J., Zekollari, H., Pellicciotti, F., & Farinotti, D. (2021). Modelling supraglacial debris-cover evolution from the single glacier to the regional scale: an application to High Mountain Asia. *The Cryosphere*. <https://doi.org/10.5194/tc-2021-233>

---

Earle, S. (2019). Physical Geology: Vol. No. 2. <https://opentextbc.ca/geology/chapter/16-2-how-glaciers-work/>

Evatt, G. W., Abrahams, I. D., Heil, M., Mayer, C., Kingslake, J., Mitchell, S. L., ... & Clark, C. D. (2015). Glacial melt under a porous debris layer. *Journal of Glaciology*, 61(229), 825-836.

Ferguson, J., & Vieli, A. (2020). Modelling steady states and the transient response of debris-covered glaciers. *The Cryosphere Discussions*, 1–31. <https://doi.org/10.5194/tc-2020-228>

Fyffe, C. L., Woodget, A. S., Kirkbride, M. P., Deline, P., Westoby, M. J., & Brock, B. W. (2020). Processes at the margins of supraglacial debris cover: Quantifying dirty ice ablation and debris redistribution. *Earth Surface Processes and Landforms*, 45(10), 2272–2290. <https://doi.org/10.1002/esp.4879>

Fyffe, C. L., Woodget, A. S., Kirkbride, M. P., Deline, P., Westoby, M. J., & Brock, B. W. (2020). Processes at the margins of supraglacial debris cover: Quantifying dirty ice ablation and debris redistribution. *Earth Surface Processes and Landforms*, 45(10), 2272–2290. <https://doi.org/10.1002/esp.4879>

Haerberli, W., & Beniston, M. (1998). Climate Change and Its Impacts on Glaciers and Permafrost in the Alps. In *Research for Mountain Area Development* (Vol. 27, Issue 4).

Hagg, W., Mayer, C., Lambrecht, A., & Helm, A. (2008). Sub-Debris Melt Rates on Southern Inylchek Glacier, Central Tian SUB-DEBRIS MELT RATES ON SOUTHERN INYLCHEK GLACIER, CENTRAL TIAN SHAN. In *Source: Geografiska Annaler. Series A, Physical Geography* (Vol. 90, Issue 1).

Hansen, J., & Nazarenko, L. (2004). Soot climate forcing via snow and ice albedos. *Proceedings of the National Academy of Sciences of the United States of America*, 101(2), 423–428. [https://doi.org/10.1073/PNAS.2237157100/SUPPL\\_FILE/7157FIG6.PDF](https://doi.org/10.1073/PNAS.2237157100/SUPPL_FILE/7157FIG6.PDF)

Inoue, J. (1977). Mass Budget of Khumbu Glacier, *Journal of the Japanese Society of Snow and Ice*, 39, 15–19, [https://doi.org/10.5331/seppyo.39.Special\\_15](https://doi.org/10.5331/seppyo.39.Special_15), 1977.

IPCC. (2021). Climate Change 2021 Working Group I contribution to the Sixth Assessment Report of the Intergovernmental Panel on Climate Change Summary for Policymakers.

Kayastha, R. B., Takeuchi, Y., Nakawo, M., & Ageta, Y. (2000). Practical prediction of ice melting beneath various thickness of debris cover on Khumbu Glacier, Nepal, using a positive degree-day factor. *Iahs Publication*, 7182.

Khan MI. (1989). Ablation on Barpu Glacier, Karakoram Himalaya, Pakistan: a study of melt processes on a faceted, debris-covered ice surface. MA thesis, Wilfrid Laurier University, Canada.

Konovalov, V. (2000). *Computations of melting under moraine as a part of regional modelling of glacier runoff* (Issue 264). IAHS Publ.

---

Kreslavsky, M. A., Head, J. W., & Marchant, D. R. (2008). Periods of active permafrost layer formation during the geological history of Mars: Implications for circum-polar and mid-latitude surface processes. *Planetary and Space Science*, 56(2), 289–302. <https://doi.org/10.1016/j.pss.2006.02.010>

le Meur, E., Gagliardini, O., Zwinger, T., & Ruokolainen, J. (2004). Glacier flow modelling: A comparison of the Shallow Ice Approximation and the full-Stokes solution. *Comptes Rendus Physique*, 5(7), 709–722. <https://doi.org/10.1016/J.CRHY.2004.10.001>

Loomis, S. R. (1970). Morphology and ablation processes on glacier ice. In *Proceedings of the Association of American Geographers* (Vol. 12, pp. 88-92).

Lüthi, M. P., Bauder, A., & Funk, M. (2010). Volume change reconstruction of Swiss glaciers from length change data. *Journal of Geophysical Research: Earth Surface*, 115(4). <https://doi.org/10.1029/2010JF001695>

Mattson, L. E. (1993). Ablation on debris covered glaciers: an example from the Rakhiot Glacier, Punjab, Himalaya. *Intern. Assoc. Hydrol. Sci.*, 218, 289-296.

Mayhew, S. (2015). A Dictionary of Geography. In *A Dictionary of Geography*. Oxford University Press. <https://doi.org/10.1093/ACREF/9780199231805.001.0001>

Mihalcea, C., Mayer, C., Diolaiuti, G., D'Agata, C., Smiraglia, C., Lambrecht, A., Vuillermoz, E., & Tartari, G. (2008). Spatial distribution of debris thickness and melting from remote-sensing and meteorological data, at debris-covered Baltoro glacier, Karakoram, Pakistan. *Annals of Glaciology*, 48, 49–57. <https://doi.org/10.3189/172756408784700680>

Mölg, N., Bolch, T., Walter, A., & Vieli, A. (2019). Unravelling the evolution of Zmuttgletscher and its debris cover since the end of the Little Ice Age. *Cryosphere*, 13(7), 1889–1909. <https://doi.org/10.5194/tc-13-1889-2019>

Nakawo, M., & Young, G. J. (1981). Field Experiments to Determine the Effect of a Debris Layer on Ablation of Glacier Ice. *Annals of Glaciology*, 2, 85–91. <https://doi.org/10.3189/172756481794352432>

Nicholson, L., & Benn, D. I. (2006). Calculating ice melt beneath a debris layer using meteorological data. <https://www.cambridge.org/core>.

Østrem, G. (1959). Ice melting under a thin layer of moraine, and the existence of ice cores in moraine ridges. *Geografiska Annaler*, 41(4), 228-230.

Pellicciotti, F., Stephan, C., Miles, E., Herreid, S., Immerzeel, W. W., & Bolch, T. (2015). Mass-balance changes of the debris-covered glaciers in the Langtang Himal, Nepal, from 1974 to 1999. *Journal of Glaciology*, 61(226), 373–386. <https://doi.org/10.3189/2015JoG13J237>

Popovnin, V. v., & Rozova, A. v. (2002). Influence of Sub-Debris Thawing on Ablation and Runoff of the Djankuat Glacier in the Caucasus Selected paper from EGS General Assembly, Nice, April-2000 (Symposium OA36). *Hydrology Research*, 33(1), 75–94. <https://doi.org/10.2166/NH.2002.0005>

---

Quincey, D. J., Luckman, A., & Benn, D. (2009). Quantification of Everest region glacier velocities between 1992 and 2002, using satellite radar interferometry and feature tracking. <https://www.cambridge.org/core>.

Ragetli, S., Bolch, T., & Pellicciotti, F. (2016). Heterogeneous glacier thinning patterns over the last 40 years in Langtang Himal, Nepal. *Cryosphere*, 10(5), 2075–2097. <https://doi.org/10.5194/tc-10-2075-2016>

Scherler, D., Bookhagen, B., & Strecker, M. R. (2011). Spatially variable response of Himalayan glaciers to climate change affected by debris cover. *Nature Geoscience* 2011 4:3, 4(3), 156–159. <https://doi.org/10.1038/ngeo1068>

Scherler, D., Wulf, H., & Gorelick, N. (2018). Global assessment of supraglacial debris-cover extents. *Geophysical Research Letters*, 45(21), 11-798.

Shroder, J. F., Bishop, M. P., Copland, L., & Sloan, V. F. (2000). Debris-Covered Glaciers and Rock Glaciers in the Nanga Parbat Himalaya, Pakistan on JSTOR. *Geografiska Annaler*, 82(No. 1), 17–31. [https://www.jstor.org/stable/521438?searchText=debris+covered+glaciers&searchUri=%2Faction%2FdoBasicSearch%3FQuery%3Ddebris%2B%2Bcovered%2Bglaciers%26so%3Drel&ab\\_segments=0%2FSYC-6292%2Fcontrol&refreqid=fastly-default%3Ab4c802998e0fa608806588283be6aa49&seq=1](https://www.jstor.org/stable/521438?searchText=debris+covered+glaciers&searchUri=%2Faction%2FdoBasicSearch%3FQuery%3Ddebris%2B%2Bcovered%2Bglaciers%26so%3Drel&ab_segments=0%2FSYC-6292%2Fcontrol&refreqid=fastly-default%3Ab4c802998e0fa608806588283be6aa49&seq=1)

Small, R. J., & Clark, M. J. (1974). The Medial Moraines of the Lower Glacier de Tsidjiore Nouve, Valais, Switzerland. *Journal of Glaciology*, 13(68), 255–263. <https://doi.org/10.1017/S0022143000023066>

Syverson KM, Mickelson DM. (1993). Ablation of debris-covered ice and the formation of pitted outwash plains at Burroughs Glacier, Southeastern Alaska. In *Proceedings of the Third Glacier Bay Science Symposium*; 66–74.

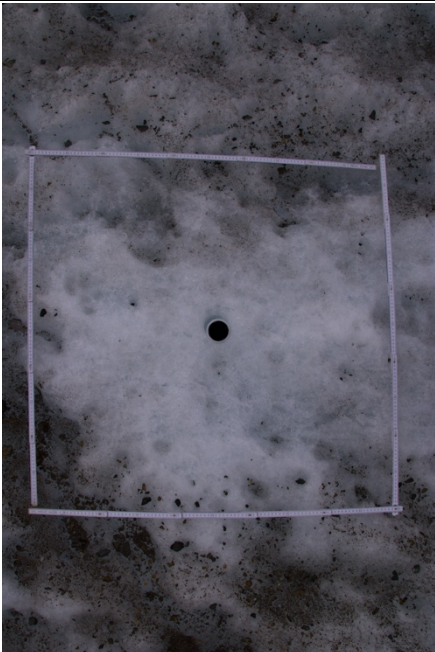
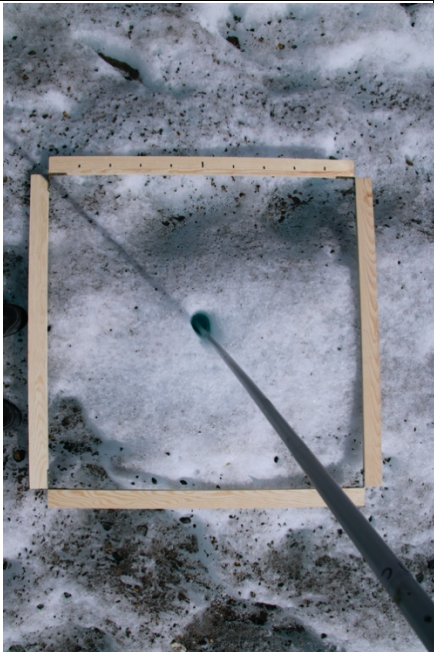

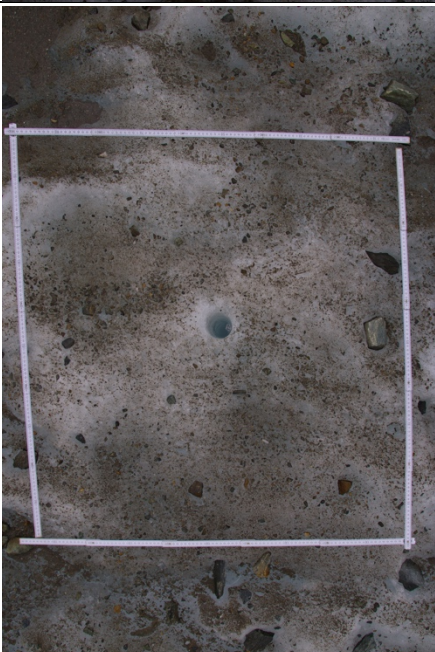

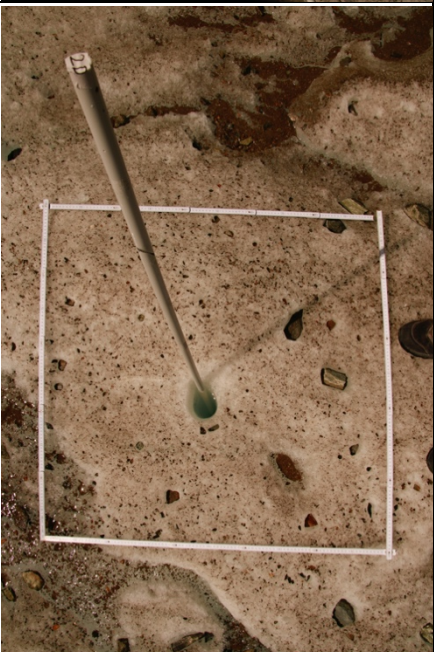
Takeuchi Y, Kayastha RB, Nakawo M. (2000). Characteristics of ablation and heat balance in debris-free and debris-covered areas on Khumbu Glacier, Nepal Himalayas, in the pre-monsoon season. *Debris-Covered Glaciers; IAHS Publication 264*: 53–61.

Westoby, M. J., Rounce, D. R., Shaw, T. E., Fyffe, C. L., Moore, P. L., Stewart, R. L., & Brock, B. W. (2020). Geomorphological evolution of a debris-covered glacier surface. *Earth Surface Processes and Landforms*, 45(14), 3431–3448. <https://doi.org/10.1002/esp.4973>



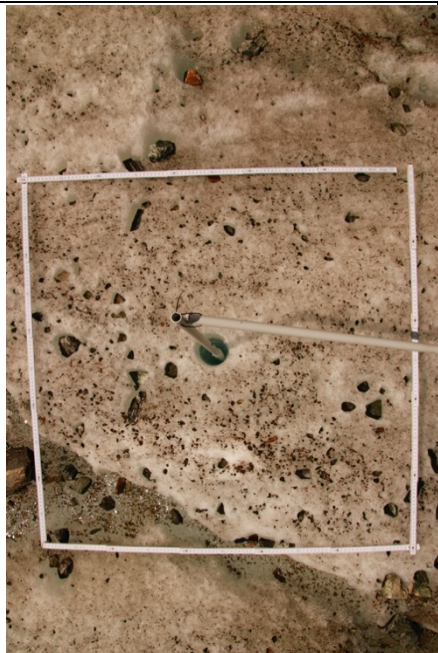
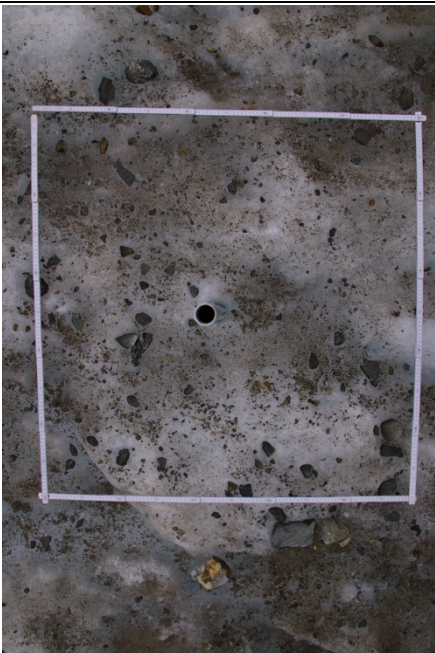
## 9 Appendix

### 9.1 Aerial photographs of the field work

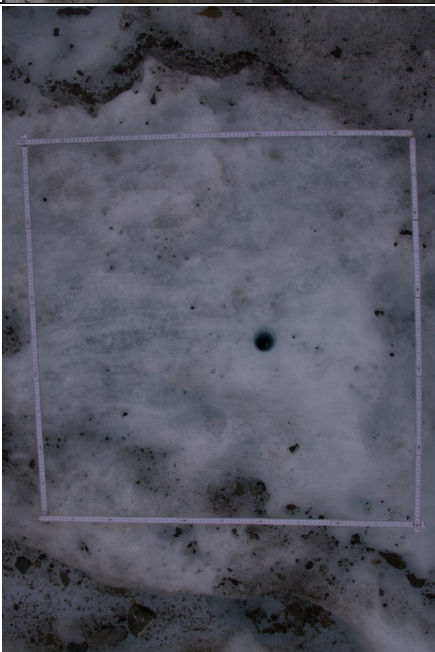
ID	11.07-14.07	20.07-22.07	5.08-6.08
1C			
2D			



3D



4C





5D



6D





7D

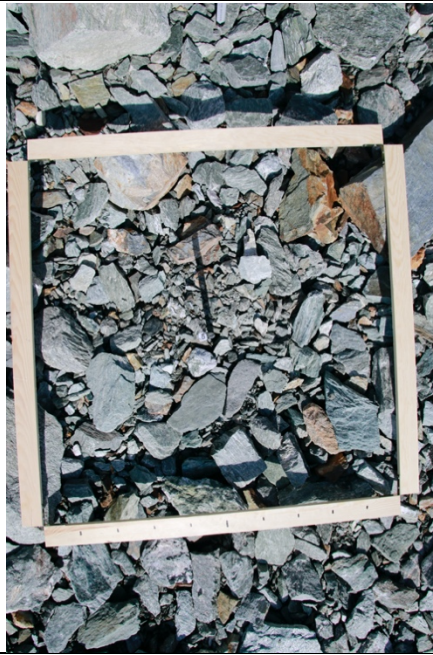


8D





9D



10  
D













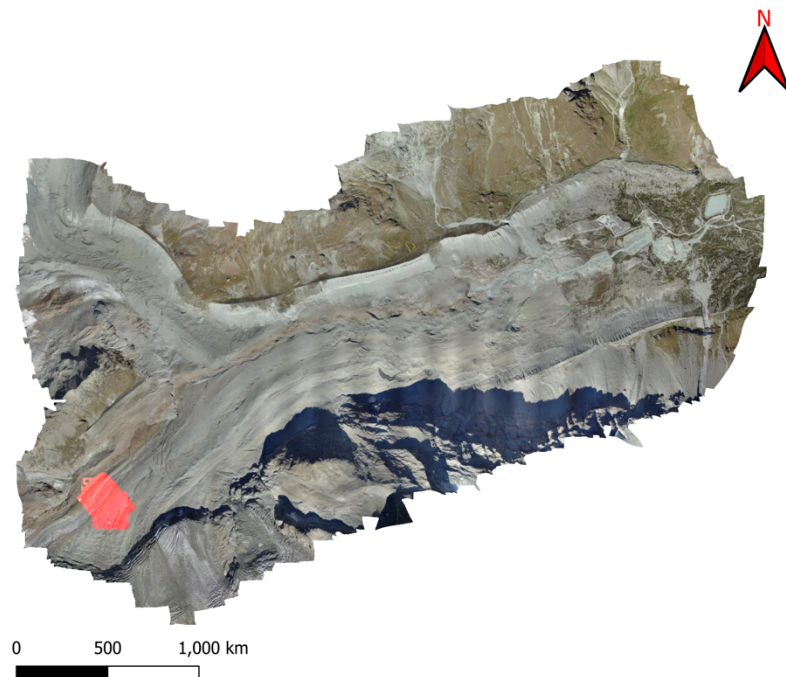




<p>15 D</p>			
<p>16 D</p>			

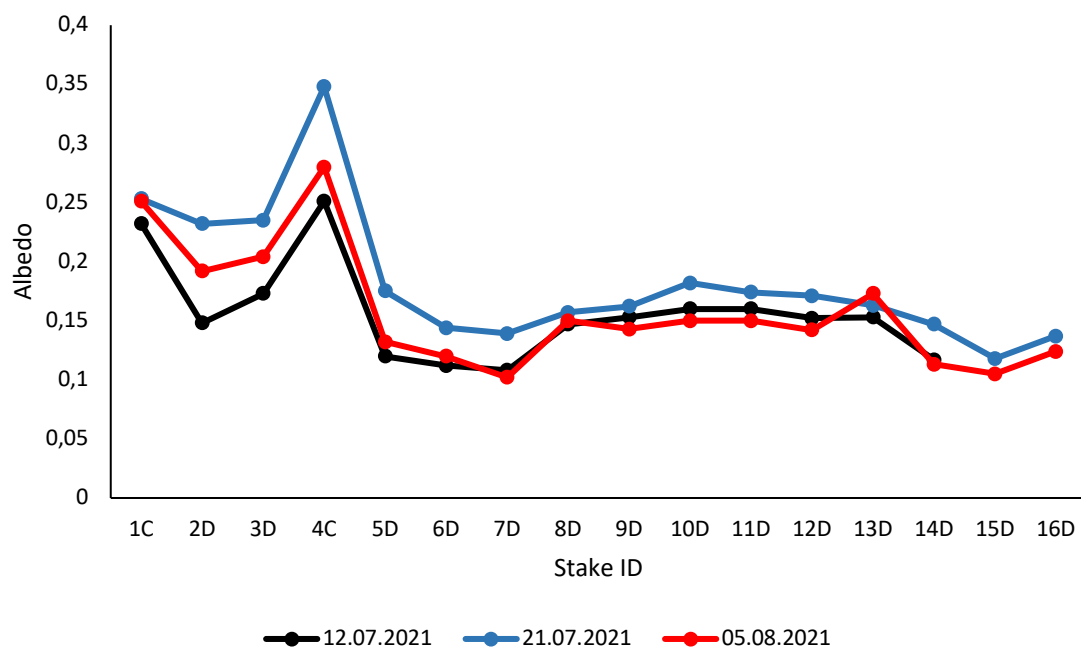
*Appendix 1. Aerial photographs of each field trip where images were taken of all 16 measurement locations.*

## 9.2 Orthophoto of the glacier



Appendix 2. Orthophoto of the ablation area of Zmuttgletscher. The red area shows where on the glacier field measurements were conducted as shown in figure 8.

## 9.3 Albedo measurements



Appendix 3. Albedo values at each ablation stake for all three measurements. Differences between the data series are due to weather conditions.

## 9.4 Melt Measurements

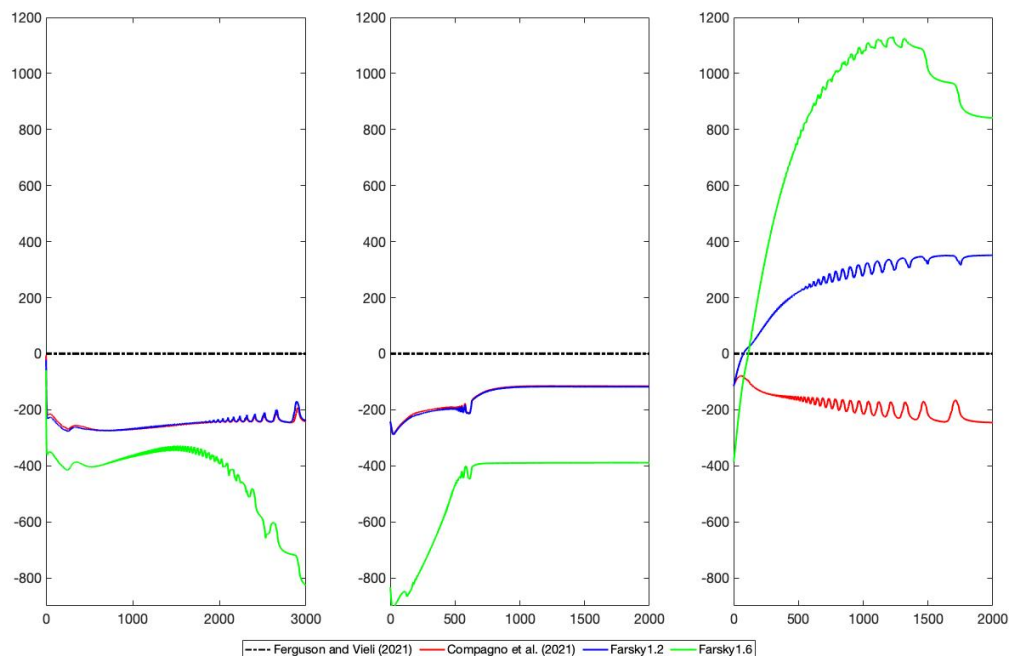
<b>Meltrate from 1st measurement to the 4th (12.07.2021 - 05.08.2021)</b>					
<b>ID</b>	<b>start measurement [cm]</b>	<b>4th measurement [cm]</b>	<b>total melt [cm]</b>	<b>melt/day [cm/d]</b>	<b>debris thickness</b>
1C	103,5	229,5	126	5,20	NA
2D	-27,25	122,5	149,75	6,19	NA
3D	104,5	244	139,5	5,76	NA
4C	-67,625	63	130,625	5,40	NA
5D	7	129,5	122,5	5,07	0,7/3,1
6D	-86,25	55	141,25	5,84	NA
7D	-87,375	66	153,375	6,35	NA
8D	7,25	93,5	86,25	3,57	5,1
9D	7,625	75	67,375	2,79	6,1
10D	7,375	66	58,625	2,43	9,1
11D	26,25	76	49,75	2,06	13,8
12D	-1,25	54,5	55,75	2,31	10,7
13D	-13,375	38,5	51,875	2,15	19,2
14D	3,25	122	118,75	4,95	2,2
15D	-3,7*	73*	76,7	5,09	2,25
16D	-1,1*	64,5*	65,6	4,36	3,5

**\*from 21.07 to 5.08**

*Appendix 4. Melt calculations for all 16 stakes.*

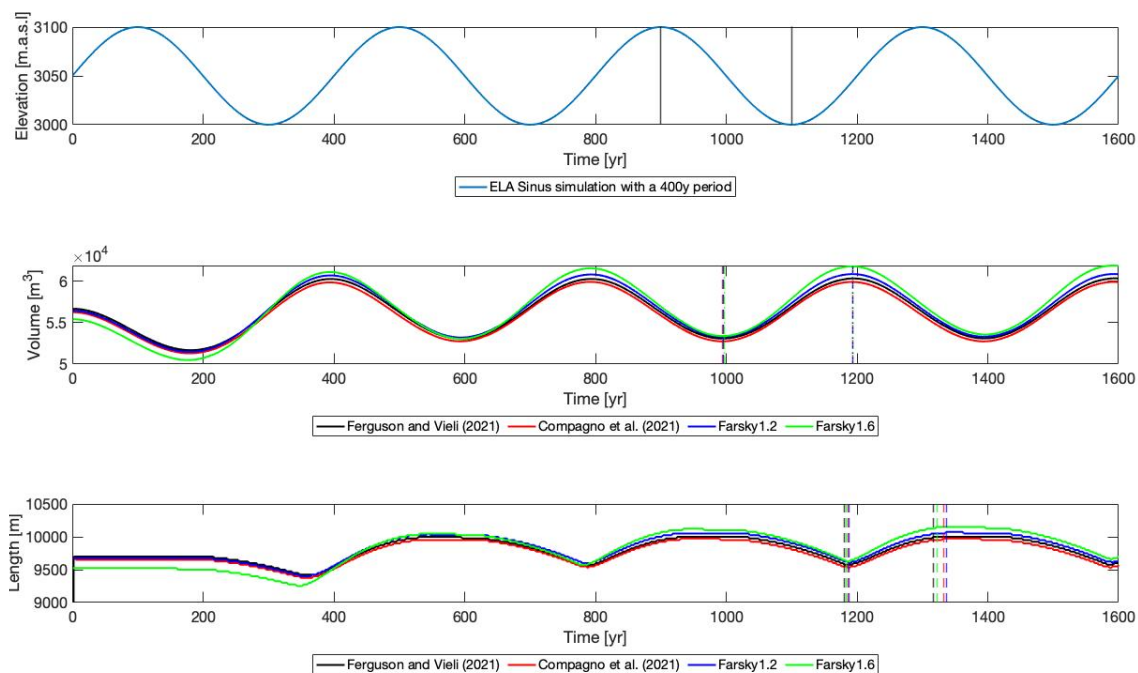


## 9.5 Relative difference between during a step change experiment

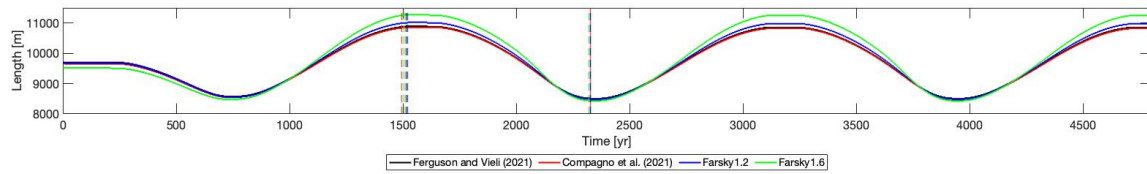
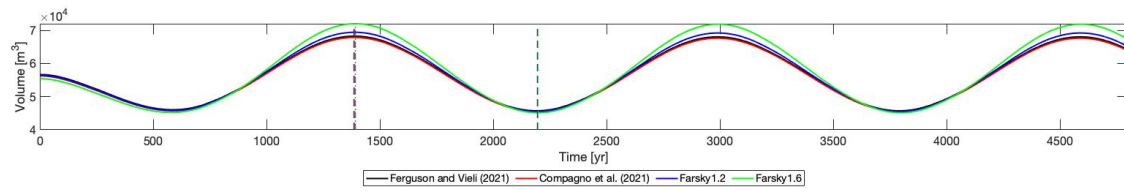
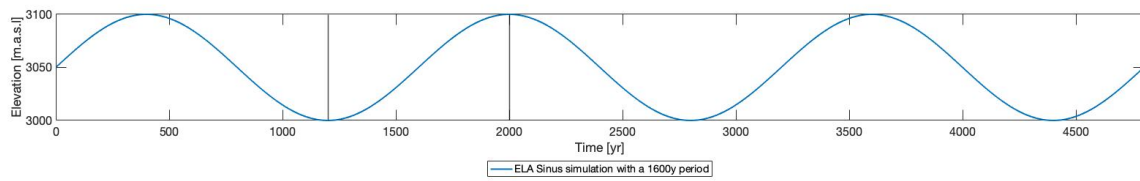


Appendix 5. Relative differences between SMB calculations with enhanced melt vs. no enhancement. Differences in (a) happen in the first 10 years where effects of enhanced melt cause a short period of decline before the debris layer increases in thickness to insulate the glacier.

## 9.6 Sinus simulations

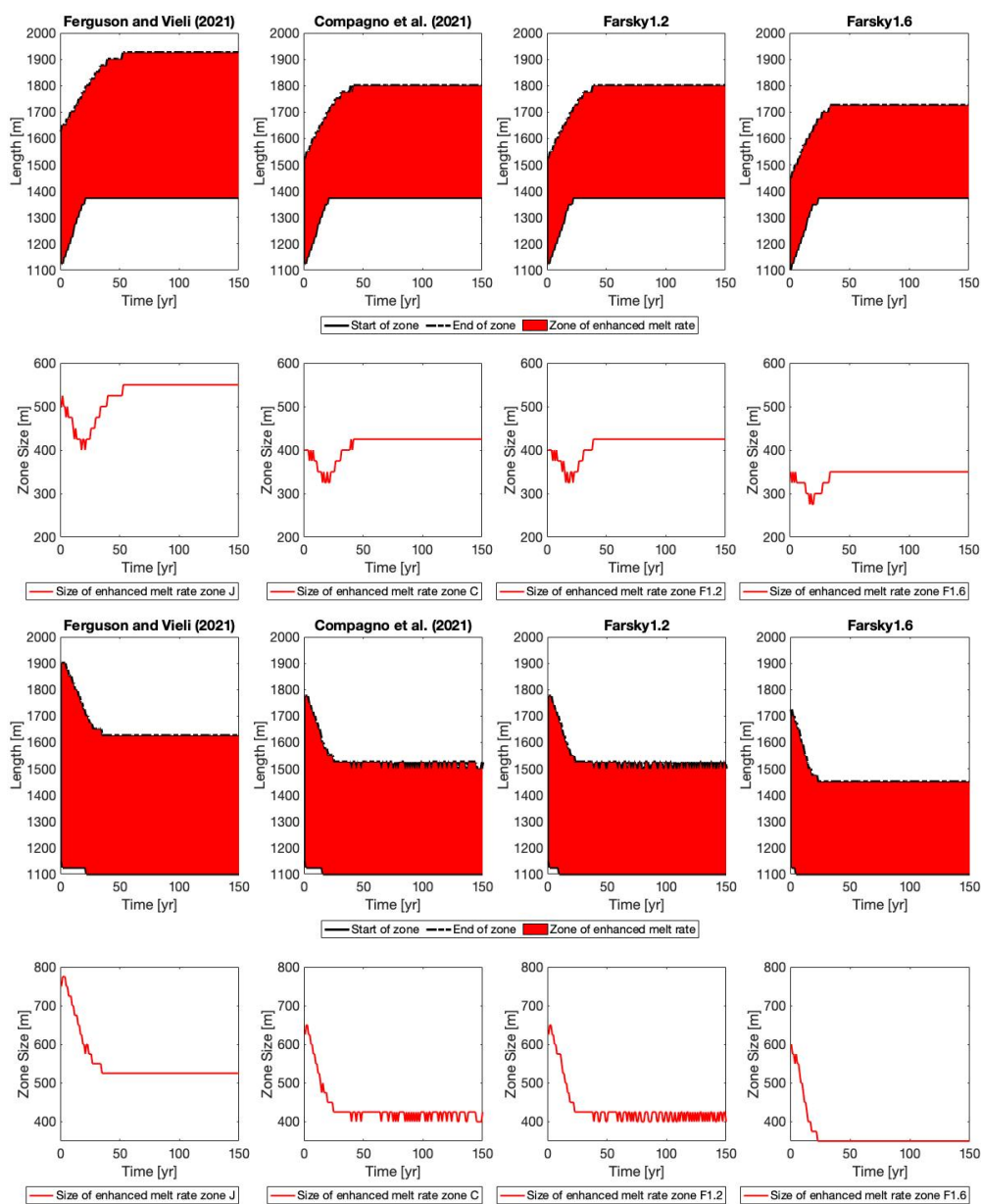


Appendix 6. Sinus simulation with a 400-year period around an ELA of 3050 m with a 50 m amplitude.



Appendix 7. Sinus simulation with a 1600-year period around an ELA of 3050 m with a 50 m amplitude.

## 9.7 Zone of enhanced melt for a glacier with a 20° glacier bed geometry



Appendix 8. Adjustment time of the zone of enhanced melt after a step change for a glacier with a 20° sloped bed geometry.

---

## Declaration of Originality

I hereby declare that the submitted thesis is the result of my own, independent work. All external sources are explicitly acknowledged in the thesis.

Zurich, 29th April, 2022

S. Farsky